

Identification of 2,4-disubstituted imidazopyridines as hemozoin formation inhibitors with fast killing kinetics and *in vivo* efficacy in the *Plasmodium falciparum* NSG mouse model

André Horatscheck[†], Ana Andrijevic[†], Aloysius T. Nchinda[†], Claire Le Manach[†], Tanya Paquet[†],
Lutete Peguy Khonde[†], Jean Dam[†], Kailash Pawar[†], Dale Taylor[‡], Nina Lawrence[‡], Christel
Brunschwig[‡], Liezl Gibhard[‡], Mathew Njoroge[‡], Janette Reader[¶], Mariëtte van der Watt[¶],
Kathryn Wicht[†], Ana Carolina C. de Sousa[^], John Okombo[^], Keletso Maepa[^], Timothy J.
Egan^{^Δ}, Lyn-Marie Birkholtz[¶], Gregory S. Basarab^{†‡}, Sergio Wittlin^{§±}, Paul V. Fish^o, Leslie J.
Street[†], James Duffy⁺, Kelly Chibale^{*†‡#Δ}

[†]Drug Discovery and Development Centre (H3D), Department of Chemistry, University of Cape
Town, Rondebosch 7701, South Africa; [‡]Drug Discovery and Development Centre (H3D),
Division of Clinical Pharmacology, University of Cape Town, Rondebosch 7701, South Africa;
[^]Department of Chemistry, University of Cape Town, Rondebosch 7701, South Africa; [#]South
African Medical Research Council, Drug Discovery and Development Research Unit,
Department of Chemistry; ^ΔInstitute of Infectious Disease and Molecular Medicine, University
of Cape Town, Rondebosch 7701, South Africa; [¶]Department of Biochemistry, Genetics and
Microbiology, Institute for Sustainable Malaria Control, University of Pretoria, Hatfield, Pretoria

0028, South Africa; [§]Swiss Tropical and Public Health Institute, Socinstrasse 57, 4002 Basel, Switzerland; [†]University of Basel, 4002 Basel, Switzerland; [°]Alzheimer's Research UK, UCL Drug Discovery Institute, The Cruciform Building, University College London, Gower Street, London WC1E 6BT, U.K.; ⁺Medicines for Malaria Venture, ICC, Route de Pré-Bois 20, PO Box 1826, 1215 Geneva, Switzerland.

KEYWORDS: Drug discovery, Malaria, cross-resistance, hERG, imidazopyridines, scaffold hop

ABSTRACT

A series of 2,4-disubstituted imidazopyridines, originating from a SoftFocus Kinase library, was identified from a high throughput phenotypic screen against the human malaria parasite *Plasmodium falciparum*. Hit compounds showed moderate asexual blood stage activity. During lead optimization, several issues were flagged such as cross-resistance against the multi-drug resistant K1 strain, *in vitro* cytotoxicity and cardiotoxicity, and were addressed through structure-activity and structure-property relationship studies. Pharmacokinetic properties were assessed in mouse for compounds showing desirable *in vitro* activity, selectivity window over cytotoxicity and microsomal metabolic stability. Frontrunner compound **37** showed good exposure in mice combined with good *in vitro* activity against the malaria parasite which translated into *in vivo* efficacy in the *P. falciparum* NOD-*scid* IL-2R γ ^{null} (NSG) mouse model. Preliminary mechanistic studies suggest inhibition of hemozoin formation as a contributing mode of action.

Introduction

Despite a reduction in mortality from 585 000 people in 2010 to 405 000 people in 2018 according to the World Health Organization (WHO) estimates, malaria remains one of the world's deadliest diseases. Children under the age of five are the most vulnerable population, especially in sub-Saharan Africa.¹ The continuous emergence of resistant *Plasmodium* parasites and mosquitoes against frontline antimalarials and insecticides, respectively, further hampers current attempts to control malaria.¹⁻³ This warrants an urgent search for new treatment options with either novel modes of action or known modes of action without cross-resistance against clinical isolates. Some of the most efficient modes of action to kill *Plasmodium* parasites as seen, for example with chloroquine, target its digestive vacuole (DV), where the parasite breaks down hemoglobin as a source of amino acids.⁴ One of the end products of this catabolic process is free heme that can oxidize to Fe(III) hemozoin, both of which are toxic to the parasite. In order to eliminate free heme, the parasite has developed a detoxification process to convert it to an insoluble crystal called hemozoin. This detoxification process is prevented by chloroquine that accumulates in the DV, binds to free heme and thereby prevents heme conversion to crystalline hemozoin. However, certain mutations in the *Plasmodium falciparum* chloroquine resistance transporter (*PfCRT*) lead to chloroquine efflux and resistance to the drug.⁵ Numerous efforts are being made to develop drugs targeting the chloroquine mode of action without being susceptible to the *PfCRT* mode of resistance.

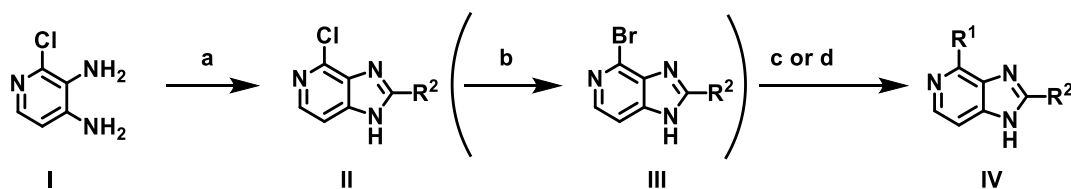
We previously reported the development of a fast-killing and highly efficacious 2,6-disubstituted imidazopyridine series from hits identified during the screening of a SoftFocus Kinase (SKF) library provided by BioFocus (now Charles River).^{6,7} We herein report the development of a fast-killing 2,4-disubstituted imidazopyridine series originating from the same screen. The new series was characterized by good *in vitro* activity against *Plasmodium falciparum* strains, high aqueous

solubility and desirable physicochemical space. Therefore, a hit-to-lead drug discovery program was initiated that successfully reduced cross-resistance seen with earlier hits of this series against the multidrug-resistant *P. falciparum* isolate K1, and significantly improved cytotoxicity and hERG margins over antiplasmodium activity. This led to the identification of lead compound **37**, which demonstrated an *in vivo* proof-of-concept in a NOD-*scid IL-2R γ ^{null}* (NSG) mouse model of *P. falciparum* infection.

Chemistry

The general synthetic route to the imidazopyridine scaffold **II** was achieved by condensing the desired benzoic acid derivatives and commercially available 2-chloro-3,4-diaminopyridine **I**, using Eaton's reagent (P₂O₅ in MeSO₃H) at 100°C for 16 hours, in good yields up to 99 % (Scheme 1). The chloro-imidazopyridine **II** was converted to the bromide **III** using phosphoryl bromide before being coupled to the corresponding amines via nucleophilic aryl substitution (S_NAr) at 140°C under microwave irradiation. In a different approach, **II** was directly converted to **IV** after being heated at 140°C with the corresponding amines in *n*-butanol in a sealed tube. Commercially available amines were used unless otherwise indicated. In the case of primary or secondary bis-amines, *tert*-butyl carbamate (Boc) or benzyl carbamate (Cbz) protected precursors were used for the S_NAr reactions. The Boc protecting group was subsequently removed under acidic conditions. The Cbz group was removed by refluxing in TFA or by hydrogenolysis.

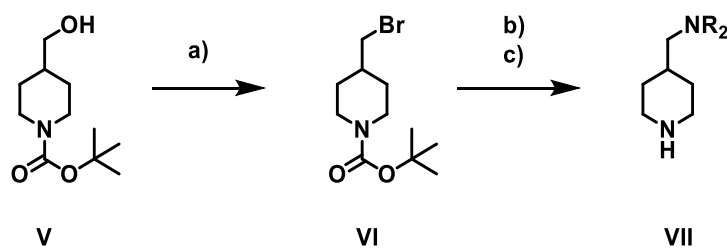
Scheme 1. General synthetic route for synthesis of the imidazopyridines



a) $R^2\text{COOH}$ ($R^2 = \text{Ar}$), Eaton's reagent, 16 h, 100 °C; b) POBr_3 , 3 h, 120 °C; c) amine (R^1), EtOH, 6 h, mw 140 °C; d) primary or secondary amine (R^1), *n*-BuOH, 16 h, 140 °C

Commercially unavailable aminomethyl-4-piperidine building blocks **VII** that were introduced onto the imidazopyridine scaffold were synthesized from the Boc protected piperidine-4-yl methanol **V** (Scheme 2). Conversion of alcohol **V** to the bromide **VI** using carbon tetrabromide and triphenylphosphine, followed by a nucleophilic substitution with the desired amine (e.g., substituted piperazines or morpholines) and the removal of the Boc-protecting group using HCl in dioxane yielded the desired building blocks. The detailed syntheses of other R^1 building blocks are described in the Supporting Information.

Scheme 2. Synthesis of aminomethyl-4-piperazine building blocks



a) CBr_4 , PPh_3 , DCM, 25 °C, 8 h; b) K_2CO_3 , HNR_2 , MeCN, 60 °C, 24 h; c) HCl/Dioxane, DCM, 25 °C, 6 h

Results and Discussion

Antiplasmodium activity, cytotoxicity, Absorption, Distribution, Metabolism and Excretion (ADME) profiling

All compounds were evaluated for antiplasmodium activity against the asexual blood stages using the drug sensitive NF54 strain of *P. falciparum*. Compounds with IC₅₀ values lower than 0.50 μM were further tested against the multidrug-(chloroquine, pyrimethamine and sulfadoxine) resistant K1 strain to check for cross-resistance. Chloroquine and artesunate were used as reference compounds in these experiments. A selection of compounds was also tested against the liver stages of the rodent parasite *P. berghei*, and early- and late-stage gametocytes of *P. falciparum* to evaluate their potential against other parasite life cycle stages.

Aqueous solubility and cytotoxicity were monitored throughout the project as they represent key parameters that can indicate limitations for either absorption from the intestines and drug safety, respectively. A benchmark for criteria to progress compounds in the different discovery stages of malaria drug development can be found on the Medicines for Malaria Venture (MMV) website.⁸ Equilibrium aqueous solubility was determined at an upper intestinal pH of 6.5 for all compounds using a miniaturized shake flask method. Compounds with aqueous solubility greater than 10 μM and *in vitro* NF54 activity lower than 0.50 μM were assessed in a 30-minute microsomal metabolic stability assay by incubating with human, rat and mouse liver microsomes. Cytotoxicity was determined in Chinese Hamster Ovary (CHO) cells for compounds with NF54 IC₅₀ values lower than 0.50 μM with the goal of identifying compounds with selective antiparasitic activity. In order to get an early assessment of potential cardiotoxicity risks, the inhibitory activity of selected compounds against the human ether-à-go-go related gene (hERG) channel was determined in a patch-clamp assay. All methods for the assays mentioned above are described further in the Supporting Information.

***In vitro* antiplasmodium activity and cytotoxicity**

Following a single point high throughput screen of a SFK library against NF54, hit compounds harboring a 2,4-disubstituted imidazopyridine scaffold, with IC_{50} values less than $0.50\ \mu\text{M}$, were identified as exemplified by **1** ($IC_{50} = 0.24\ \mu\text{M}$) and **2** ($IC_{50} = 0.49\ \mu\text{M}$, Figure 1). Amongst these, R^1 groups containing a basic aliphatic functionality were a common feature, and derivatives with 3,4-difluorophenyl and 3-trifluoromethoxyphenyl groups at the R^2 position had the highest activity.

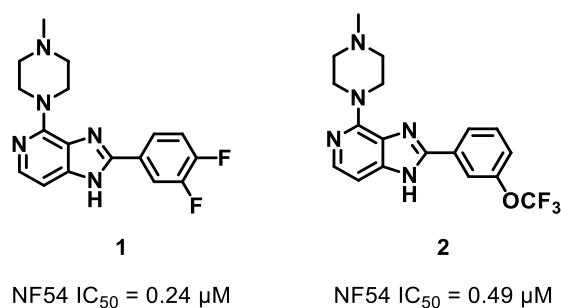


Figure 1. Hit compounds **1** and **2** from a phenotypic screen against the asexual blood stages of *P. falciparum*

Studies to determine the minimum pharmacophore (Table 1) showed that a basic functionality on the R^1 substituent predicted to be protonated at physiological pH was beneficial for NF54 activity as seen for morpholine **4** and piperazinone **3** with considerably weaker activity (NF54 $IC_{50} = 3.1\ \mu\text{M}$ and $> 10\ \mu\text{M}$, respectively) relative to the hit piperazine **1** (NF54 $IC_{50} = 0.24\ \mu\text{M}$). The basicity of the pyridine nitrogen in the scaffold also appeared to be beneficial for activity. Hence, removing the nitrogen that links the substituent to the scaffold as with **5** (NF54 $IC_{50} > 10\ \mu\text{M}$) abolished activity at the highest concentration tested (compare to **6**, NF54 $IC_{50} = 0.17\ \mu\text{M}$). The change from R^1 being amino to alkyl was predicted to decrease the pK_a of the scaffold pyridine nitrogen from 8.3 to 5.5 (ACD Labs Percepta v 2019.1.3), which could explain the loss of activity.

Further structure-activity-relationship (SAR) supports the importance of the scaffold pK_a: the pyrrolopyridines with a measured pK_a one log unit higher than the imidazopyridines (pK_a ~8 vs ~7) were slightly more active (Supporting Information, Table S1). It should be noted, however, that the predicted pK_a of the imidazopyridines is more than one log unit higher than the measured values demonstrating the limitations of the calculations. Nonetheless, the calculations can be useful for estimating relative pK_a values within an analogue series. Substituted R¹ piperazines having slightly larger substituents such as the pyrrolidopiperazine **7** (NF54 IC₅₀ = 0.22 μM), and the hydroxyethyl derivative **8** (NF54 IC₅₀ = 0.57 μM) maintained activity, unless their basicity was lowered by the substituent as with the trifluoroethyl analogue **9** (NF54 IC₅₀ = 2.3 μM) and the *N*-phenyl analogue **10** (NF54 IC₅₀ > 1 μM). *N*-demethylation of **1** did not have a significant effect (**6**: NF54 IC₅₀ = 0.17 μM) on activity.

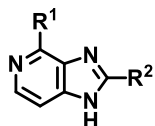
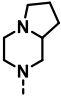
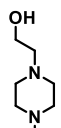
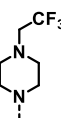
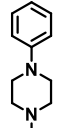


Table 1. Studies to determine the minimum pharmacophore at the R¹ substituent

Entry	R ¹	R ²	NF54 IC ₅₀ (μM) ^a	K1 IC ₅₀ (μM) ^a	aq. solubility pH 6.5 (μM)	CHO CC ₅₀ (μM) ^b
1			0.24	0.50	130	> 50
3			> 10	-	< 5	-
4			3.1	-	-	-
5			> 10	-	200	-
6			0.17	0.97	150	8.1

7		0.22	0.48	120	32
8		0.57	1.4	95	-
9		2.3	-	10	39
10		> 1	-	-	-

^a Mean from 3 values of ≥ 2 independent experiments with multidrug resistant (K1) and sensitive (NF54) strains of *P. falciparum* using the parasite lactate dehydrogenase (pLDH) assay. The majority of the individual values varied less than $2\times$ (maximum $3\times$). A set of compounds was confirmed in the [^3H]-hypoxanthine incorporation assay. ^b Mean of 3 values performed on one occasion. Individual replicates varied less than $2x$.

After establishing that a basic center was required for activity, SAR studies on the R^1 substituent were further expanded (Table 2). The addition of methyl groups to obtain 3,5-dimethyl piperazine derivative **11** (NF54 $\text{IC}_{50} = 0.076 \mu\text{M}$) led to the first compound with sub 100 nanomolar activity, while its *N*-methyl analogue **12** (NF54 $\text{IC}_{50} = 0.26 \mu\text{M}$) was significantly less active. Interestingly, this trend was reversed when expanding the six-membered piperazine ring to a seven-membered diazepane ring. The desmethyl diazepane **13** (NF54 $\text{IC}_{50} = 0.21 \mu\text{M}$) was significantly less active than the methylated (**14**, NF54 $\text{IC}_{50} = 0.061 \mu\text{M}$), cyclopropylmethyl (**15**, NF54 $\text{IC}_{50} = 0.020 \mu\text{M}$) and bridged tricyclic (**16**, NF54 $\text{IC}_{50} = 0.079 \mu\text{M}$) analogues. Relative to the initial hit compound **1**, the cyclopropylmethyl diazepane **15** gained more than 10-fold activity while maintaining high aqueous solubility at pH 6.5 ($200 \mu\text{M}$) and low *in vitro* cytotoxicity ($\text{CC}_{50} = 17 \mu\text{M}$) resulting in a selectivity index (SI) of 850 over NF54 activity.

One drawback of this series became evident as cross-resistance was observed in the multidrug-resistant K1 strain where IC_{50} values were 4-fold or higher compared to NF54. For example, the 4-aminopiperidine **25** showed a cross-resistance ratio of 16 (NF54 IC_{50} = 0.073 μ M, K1 IC_{50} = 1.2 μ M for a K1/NF54 = 16) comparable to chloroquine (K1/NF54 = 35). Minimizing the activity shift between drug sensitive and drug resistant strains is important for potential clinical utility since clinically used antimalarial drugs must be active against drug-resistant strains. A higher IC_{50} for a given field isolate would require a higher drug dose and a higher blood exposure, which in turn would increase the probability of adverse effects. The mechanistic reason for the variable cross-resistance in this series is unknown, but the working hypothesis was that drug resistance occurred due to efflux of certain chemotypes, e.g. by *Pf*CRT, and could be overcome by structural modifications. Comparison of cross-resistance ratios in tertiary, secondary and primary amines highlighted that the cross-resistance ratio in tertiary amines, such as methylpiperazine **1** (K1/NF54 = 2.1), diazepanes **14** (K1/NF54 = 1.6) and **15** (K1/NF54 = 3.9), and piperaziny-4-piperidine **30** (K1/NF54 = 1.4) was lower compared to their des-alkyl secondary amine analogues **6** (K1/NF54 = 5.7), **13** (K1/NF54 = 5) and **31** (K1/NF54 = 13). *N*-Dimethylation of the 4-aminopiperidine **25** to give **26** led to a reduction in the cross-resistance ratio from 16 to 1.1, with only a minimal loss in activity (NF54 IC_{50} = 0.14 μ M). Furthermore, the insertion of a methylene group in **25** (K1/NF54 = 16) to obtain **28** (NF54 IC_{50} = 0.068 μ M, K1/NF54 = 2.8), thereby pushing out the distal basic center, also significantly reduced the cross-resistance ratio whilst maintaining activity. Encouraged by these observations, we focused on the aminopiperidine derivatives that displayed overall favorable properties for further optimization. The diazepane analogues (e.g. **14**) were discontinued due to microsomal metabolic instability (mouse liver microsomes (MLM) $CL_{int,app}$ =

145 $\mu\text{l}/\text{min}/\text{mg}$) and hERG inhibitory potency (hERG $\text{IC}_{50} = 0.4 \mu\text{M}$), (see Supporting Information, Tables S1 and S5).

A successful strategy to reduce cross-resistance and improve NF54 activity was the extension of the basic center by introducing a *N*-methylpiperazine substituent on the aminopiperidine creating the piperazinylpiperidine of **27** and **18** (NF54 $\text{IC}_{50\text{s}} = 0.064 \mu\text{M}$ and $0.046 \mu\text{M}$ respectively). However, cytotoxicity margins for the latter compounds were low (SI = 47-110). Based on the promising activity and cross-resistance trends of the aminomethyl-piperidine **28** and the gains of activity observed by addition of a piperazine leading to **27**, the corresponding methyl piperazine analogues **22** and **29** were synthesized and shown to possess significantly higher activity with NF54 IC_{50} values of less than $0.020 \mu\text{M}$ and comparable values against K1. Further SAR studies indicated that modulation of basicity could improve cytotoxicity margins, as exemplified by the morpholine **24** that exhibited only a slight loss in activity (NF54 $\text{IC}_{50} = 0.051 \mu\text{M}$) whilst cytotoxicity margins improved from 370-fold for piperazine **22** to 690-fold.

The inversed piperidinylpiperazine **19** was nearly equipotent and showed higher cytotoxicity margins ($\text{CC}_{50} = 33 \mu\text{M}$, SI = 460) compared to **27** ($\text{CC}_{50} = 3.0 \mu\text{M}$) and **18** ($\text{CC}_{50} = 5.0 \mu\text{M}$). In addition, **19** displayed the lowest intrinsic clearance in a mouse PK study (see section further below) compared to other compounds. As mentioned, alkylation of diazepanes increased activity as opposed to methylation of piperazines, which decreased activity, and the addition of a distant basic center was beneficial for NF54 activity and hERG (see section below). Hence, a diazepane was used as a linker leading to **20** with the goal to combine these positive trends. While the activity and the cytotoxicity margin for **20** were high (NF54 $\text{IC}_{50} = 0.035 \mu\text{M}$, SI = 490), microsomal stability ($\text{MLM CL}_{\text{int,app}} > 200 \mu\text{l}/\text{min}/\text{mg}$) was still low. The attempt to improve microsomal stability by lowering the electron density in the diazepane through the introduction of fluorines

(**21**: NF54 IC₅₀ = 0.059 μM, CC₅₀ = 33 μM) led to significant improvements (MLM CL_{int,app} = 33 μl/min/mg), albeit not sufficiently so for progression towards an optimized lead.

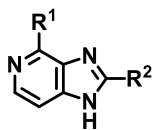
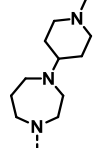
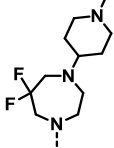
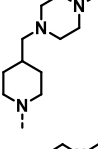
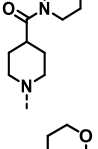
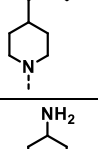
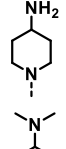
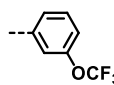
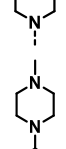
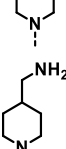
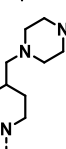
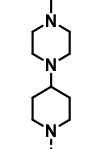


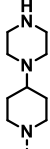


Table 2. SAR and SPR studies with variations on the R¹ substituent

Entry	R ¹	R ²	NF54 IC ₅₀ (μM) ^a	K1 IC ₅₀ (μM) ^a	aq. solubility pH 6.5 (μM)	CHO CC ₅₀ (μM) ^b
11			0.076	0.45	190	6.5
12			0.26	0.72	50	>50
13			0.21	1.0	165	7.2
14			0.061	0.10	170	14
15			0.020	0.077	200	17
16			0.079	0.43	200	28
17			0.11	0.91	200	8.2
18			0.046	0.22	130	5.0
19			0.071	0.26	200	33

20			0.035	0.22	200	17
21			0.059	0.16	180	33
22			< 0.020	0.027	195	7.4
23			0.10	0.38	200	>50
24			0.051	0.12	85	35
<hr/>						
25			0.073	1.2	200	42
26			0.14	0.19	180	
27			0.064	0.091	190	3.0
28			0.068	0.19	200	2.9
29			< 0.020	0.012	200	0.95
<hr/>						
30			0.058	0.080	195	4.8

31		0.036	0.46	200	34
Chloroquine		0.008	0.28	-	-

^a Mean from 3 values of ≥ 2 independent experiments with multidrug resistant (K1) and sensitive (NF54) strains of *P. falciparum* using the parasite lactate dehydrogenase (pLDH) assay. The majority of the individual values varied less than $2\times$ (maximum $3\times$). A set of compounds was confirmed in the [³H]-hypoxanthine incorporation assay. ^b Mean of 3 values performed on one occasion. Individual replicates varied less than $2x$.

In order to further assess the influence of R² substitution on antiplasmodium activity and improve the cytotoxicity SI, the most promising R¹ substituents in terms of activity, piperazinylpiperidine **27**, and piperazinylmethylpiperidine **29**, were used to explore different R² substituents (Table 3). In general, electron-withdrawing substituents on R² such as fluorine (e.g. **18**, **32**, **30**, **38**), nitrile (**33**) and ester (**35**) showed high NF54 activity with IC₅₀ values of less than 0.1 μ M. The saturated cyclopentanes of **36** and **44** (NF54 IC₅₀ > 10 μ M and 9.3 μ M, respectively) and more polar substituents, such as the amide of **41** (NF54 IC₅₀ = 1.0 μ M), the amine of **42** (NF54 IC₅₀ = 2.2 μ M) and the carboxylic acid of **43** (NF54 IC₅₀ > 10 μ M), were detrimental to activity.

Interestingly, the R² substitution pattern had a significant impact on cytotoxicity. While 3-trifluoromethoxy- and 3,4-difluorophenyl derivatives **27**, **29**, **18** and **22** displayed low cytotoxicity margins (SI ranging from 47-370), the 3,5-difluorophenyl analogues exemplified by **37** showed an improvement (SI = 1040) while retaining good NF54 activity (IC₅₀ = 0.023 μ M).

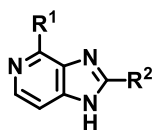
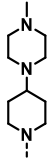
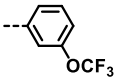
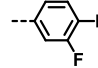
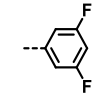
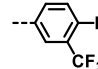
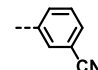
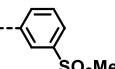
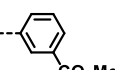
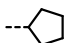
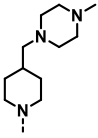
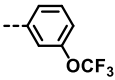
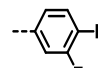
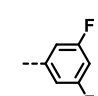
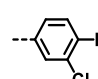
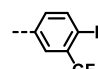
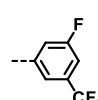
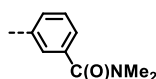
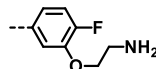
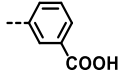
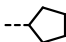


Table 3. SAR exploration of the R² substituent

Entry	R ¹	R ²	NF54 IC ₅₀ (μM) ^a	K1 IC ₅₀ (μM) ^a	aq. solubility pH 6.5 (μM)	CHO CC ₅₀ (μM) ^b
27			0.064	0.091	190	3.0
18			0.046	0.22	130	5.0
32			0.050	0.17	200	30
30			0.058	0.080	195	4.8
33			0.11	0.58	-	16
34			0.45	1.5	190	> 50
35			0.079	0.28	-	34
36			> 10	-	170	-
29			< 0.020	0.012	200	0.95
22			< 0.020	0.027	195	7.4
37			0.023	0.041	200	24
38			< 0.012	0.025	155	0.85
39			0.050	0.017	165	3.1
40			0.054	0.089	165	3.1
41			1.0	-	180	> 50
42			2.2	-	200	-

43		> 10	-	195	> 50
44		9.3	-	< 5	-

^a Mean from 3 values of ≥ 2 independent experiments with multidrug resistant (K1) and sensitive (NF54) strains of *P. falciparum* using the parasite lactate dehydrogenase (pLDH) assay. The majority of the individual values varied less than $2\times$ (maximum $3\times$). A set of compounds was confirmed in the [³H]-hypoxanthine incorporation assay. ^b Mean of 3 values performed on one occasion. Individual replicates varied less than $2x$.

Keeping the R² 3,5-difluorophenyl substituent constant, further variations of the R¹ substituent investigated different linkers (Table 4), such as the 1,4-diaminohexyl linkers in compounds **46** and **47**, as well as 3-position piperazinomethylpiperidines of **48** and **49**. Several derivatives with modulated basicity in the R¹ substituent were also synthesized. However, derivatives with replacements of the piperazine without a distal basic center, such as thiomorpholinedioxide **50** (NF54 IC₅₀ = 1.4 μ M), difluoropiperidine **51** (NF54 IC₅₀ = 0.20 μ M), morpholine **52** (NF54 IC₅₀ = 0.29 μ M) and spiromorpholine **54** (NF54 IC₅₀ = 0.18 μ M) were detrimental to activity, further highlighting the importance of the distal basic center. *N*-trifluoroethylated derivative **53** maintained NF54 activity below 0.1 μ M despite the expectation that the distal piperazine nitrogen would not be protonated at physiological pH. Bulkier modifications on the distal piperazine nitrogen, such as *tert*-butyl and methylimidazole (**56** and **55**), maintained activity and high aqueous solubility. The cytotoxicity margin for **55** (SI = 1140) was on par with the methyl substituted derivative **37** making it interesting for further *in vivo* studies.

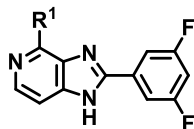
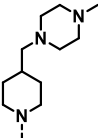
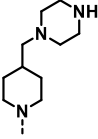
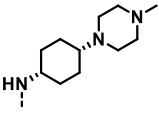
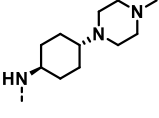
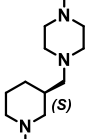
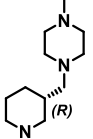
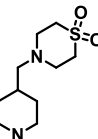
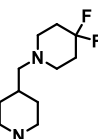
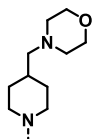
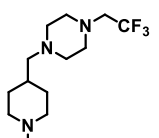
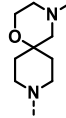
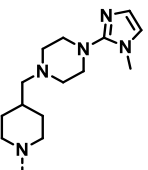
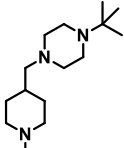


Table 4. Activity and cytotoxicity of compounds with 3,5-difluorophenyl R² substituent

Entry	R ¹	NF54 IC ₅₀ (μM) ^a	K1 IC ₅₀ (μM) ^a	aq. solubility pH 6.5 (μM)	CHO CC ₅₀ (μM) ^b
37		0.023	0.041	200	24
45		0.038	0.24	190	20
46		0.16	0.31	200	14
47		0.13	0.24	200	11
48		0.028	0.13	145	3.2
49		0.073	0.17	200	7.9
50		1.4	-	< 5	> 50
51		0.20	0.31	< 5	26
52		0.29	0.39	25	> 50
53		0.075	0.16	180	40

54		0.18	0.32	175	32
55		0.029	0.053	135	33
56		0.019	0.047	185	8.6

^a Mean from 3 values of ≥ 2 independent experiments with multidrug resistant (K1) and sensitive (NF54) strains of *P. falciparum* using the parasite lactate dehydrogenase (pLDH) assay. The majority of the individual values varied less than $2\times$ (maximum $3\times$). A set of compounds was confirmed in the [³H]-hypoxanthine incorporation assay. ^b Mean of 3 values performed on one occasion. Individual replicates varied less than $2x$.

Encouraged by the favorable profile of **37**, including high NF54 and K1 activity and an excellent cytotoxicity margin, changes to the scaffold imidazopyridine were investigated while maintaining the R¹ and R² substituents of **37** with the aim of improving PK properties (shown later for select compounds), as shown in Table 5. Omission of the pyridine nitrogen of the scaffold as for the benzimidazole **57** was detrimental to activity (NF54 IC₅₀ = 0.83 μ M), while replacement of one of the imidazole nitrogens with a carbon atom, exemplified by pyrrolopyridine **58** (NF54 IC₅₀ = 0.014 μ M), maintained high activity. Methylation at the N¹-position as in **59** was detrimental (NF54 IC₅₀ > 3.0 μ M) to activity. None of the scaffold modifications, such as the isomeric **60** and **61** or the pyridazine **64** and the pyrimidine **65** (NF54 IC₅₀ values between 0.13 and 1.8 μ M) led to any improvements in activity. There was a 2-fold improvement in NF54 activity for the 6-Me analogue **62** (IC₅₀ = 0.012 μ M) over **37**; however, the cytotoxicity margin (SI = 160) was lower.

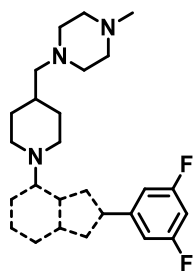


Table 5. SAR studies on scaffold changes to the imidazopyridine core.

Entry	Core	NF54 IC ₅₀ (μ M) ^a	K1 IC ₅₀ (μ M) ^a	aq. solubility pH 6.5 (μ M)	CHO CC ₅₀ (μ M) ^b	hERG IC ₅₀ (μ M)
37		0.023	0.041	200	23	> 30
57		0.83	1.5	200	22	> 30
58		0.014	0.092	140	2.6	5
59		> 3	-	150		
60		0.13	0.33	125	46	
61		0.53	-	< 5		
62		0.012	0.021	200	1.9	> 30
63		0.077	0.049	< 5		
64		0.58	2.9	190		
65		1.8	-	55		

^a Mean from 3 values of ≥ 2 independent experiments with multidrug resistant (K1) and sensitive (NF54) strains of *P. falciparum* using the parasite lactate dehydrogenase (pLDH) assay. The majority of the individual values varied less than 2 \times (maximum 3 \times). A set of compounds was confirmed in the [³H]-hypoxanthine incorporation assay. ^b Mean of 3 values performed on one occasion. Individual replicates varied less than 2x.

hERG activity

As hERG activity has been determined for a variety of compounds and served as an indicator of potential cardiotoxicity risks, we set out to identify the chemical features that mitigated its activity (Supporting Information, Table S1).⁹ Herein, it was found that hERG activity was mainly influenced by substitution changes on the scaffold and on the R¹ substituent.

While the scaffold change from imidazopyridine to pyrrolopyridine had little impact on NF54 activity, hERG activity was up to 7-fold higher for the pyrrolopyridines (compare hERG IC₅₀s of imidazopyridines/pyrrolopyridines, e.g. **23/S2**: 12 μM / 3 μM; **32/S5**: > 30 μM / 4 μM and **37/S8**: > 30 μM / 5 μM) (see Supporting Information, Table S1). It is noteworthy that pyrrolopyridines in general showed a higher measured pK_a for the core, as exemplified by pyrrolopyridine **S7** (pK_a = 8.2) versus imidazopyridine **S6** (pK_a = 7.4) suggesting that the higher basicity of the core heterocycle increased hERG binding. Relative to the R¹ substituent wherein there is a second basic moiety, diazepanes (e.g. **14** and **S4**) as well as the structurally similar piperazine **6** showed low hERG IC₅₀ values (0.4 μM, 0.4 μM and 3.4 μM, respectively), which led to their deprioritization. In general, R¹ substituents with a second protonation site closer to the core (e.g. **14**, **24**, **53**, **S8**; all with hERG IC₅₀s ≤ 3 μM) had a higher hERG liability compared to compounds with a protonation site further away from the core (e.g. **32** and **37**, all > 30 μM).

Overall, hERG activity was lowest for imidazopyridine compounds with a protonation site on the R¹ substituent further away from the core. As **37** (hERG IC₅₀ > 30 μM) showed the highest hERG margin (> 1300-fold over the NF54 strain) along with high NF54 activity and a high SI relative to cytotoxicity, it was selected for advanced profiling as a frontrunner compound (see below).

Parasitological and life cycle profiling of selected compounds

The frontrunner compound **37** was shown to be fast acting without lag time in a parasite reduction ratio (PRR) assay¹⁰ at 10 x IC₅₀ exhibiting a 4.9 log reduction of parasitemia within the 48h life cycle of *P. falciparum* (Figure 2). This boded well for the compound and the series, as fast killing kinetics of the asexual blood stage parasites in the clinical setting are key to a fast relief of symptoms.

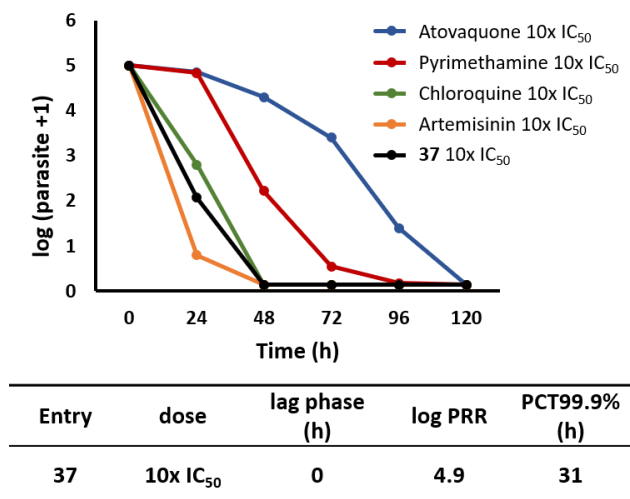


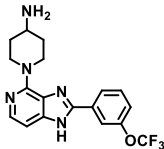
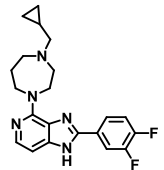
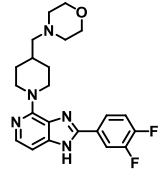
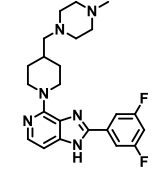
Figure 2. Results of the *in vitro* parasite reduction ratio (PRR) assay for **37** in comparison to known antimalarials.

Profiling of **37** against a panel of lab generated resistant mutants less susceptible to antimalarials in clinical development showed no signs of cross-resistance (see Supporting Information, Table S3). Hence, its mode of action or mode of resistance most likely differs from those ascribed to the other compounds of Table S3 including inhibition of or binding to *Pf* eukaryotic elongation factor 2 (*PfeEF2*)¹¹, *Pf* phosphatidylinositol-4-kinase (*PfPI4K*)¹², *Pf* dihydroorotate dehydrogenase (*PfDHODH*)¹³, *Pf* cyclic amine resistance locus (*Pfcarl*)¹⁴, and *Pf* cytochrome B (*PfcytB*)¹⁵. While

there is no information on the clinical relevance of these lab mutants, it was encouraging to see that they were equally susceptible to the tested imidazopyridine. In addition, no cross-resistance was found when tested against a panel of clinical field isolates (see Supporting Information, Table S4) though the higher IC_{50} against the K1 strain sets a potential bar for which coverage would be needed for **37** in the clinical setting. When **37** was assessed against a synchronized culture of asexual parasites, it showed comparable activity on the ring and schizont stages ($IC_{50} = 0.027 \mu\text{M}$ and $0.060 \mu\text{M}$, respectively), similar to what is observed for chloroquine.¹⁶

Four compounds, including frontrunner **37**, were selected for profiling against the liver and transmissible sexual gametocyte stages of the *Plasmodium* parasite life cycle (Table 6) in order to assess their potential for prophylaxis and transmission blocking, respectively. Data from the early-stage (stage I-III) and late-stage (stage IV/V) sexual gametocytes were obtained from *P. falciparum*. Liver stage data was obtained from the rodent parasite *P. berghei in vitro* assay.¹⁷ While all of the compounds showed liver stage activity, only **24** showed a lower IC_{50} of $0.29 \mu\text{M}$ that was within 6-fold of its NF54 IC_{50} . With respect to the transmission stages¹⁸, all of the compounds only showed weak to moderate activity against early- and late-stage gametocytes with **25** being most notable (stage I-III $IC_{50} = 0.78 \mu\text{M}$ and stage IV/V $IC_{50} = 2.8 \mu\text{M}$). Interestingly, the relative activities against the different life cycle stages can differ quite significantly for each compound. **37** only showed high activity against the asexual stages of the parasite life cycle, therefore showing a similar profile to chloroquine in PRR¹⁰, stage specificity¹⁹ and life cycle activity²⁰, albeit cross-resistance to chloroquine-resistant strains was minimal.

Table 6. Activity of selected compound against the *Plasmodium* life cycle: asexual blood stage (ABS), liver stage (*Pb* sporozoite), stage I-III (early) and stage IV/V (late) gametocytes

Entry	Structure	ABS NF54 IC ₅₀ (μM) ^a	Pb sporozoite IC ₅₀ (μM)	Stage I-III gametocyte IC ₅₀ (μM) ^b	Stage IV/V gametocyte % inhibition (5 μM)
25		0.073	14	0.78	95 (IC ₅₀ = 2.8 μM)
15		< 0.020	17	5.3	48
24		0.051	0.29	1.3	0
37		0.023	14	n.a.	31

n.a. = not active (< 50% inhibition at 5 μM); ^a Mean from 3 values of ≥2 independent experiments with multidrug resistant (K1) and sensitive (NF54) strains of *P. falciparum* using the parasite lactate dehydrogenase (pLDH) assay. The majority of the individual values varied less than 2× (maximum 3×). A set of compounds was confirmed in the [³H]-hypoxanthine incorporation assay. ^b Mean of 3 technical replicates using the luciferase assay. The individual values varied less than 2x.

In view of the aforementioned profile similarity to chloroquine, investigation of chloroquine-related inhibition of hemozoin formation for **37** was carried out using a β-hematin (βH) inhibition assay.²¹ This assay uses pyridine to detect unreacted hematin during the formation of synthetic hemozoin (β-hematin) mediated by the detergent Nonidet P-40 and offers a robust method to find

β -hematin formation inhibitors as a surrogate to what occurs in the digestive vacuole (DV) of the parasite. Herein, **37** showed an IC_{50} of 24 μ M comparable to chloroquine ($IC_{50} = 21 \mu$ M). Basic compounds targeting the processes in the DV presumably accumulate to high concentrations in this acidic vacuole via pH trapping. Therefore, both pH trapping and hemozoin inhibition may contribute to NF54 activity. As a consequence, the core pyridazine analogue **64** without a basic core nitrogen was equipotent in the β -hematin assay ($IC_{50} = 25 \mu$ M), where compound accumulation is not a requirement for potency, while being 25-fold less active against whole cell NF54 parasites. Despite having an electron withdrawing group adjacent to the core nitrogen, the nitrile derivative **63** maintained reasonable NF54 activity ($IC_{50} = 0.077 \mu$ M), which may be a result of its greater ability to inhibit hemozoin formation (β H $IC_{50} = 8.5 \mu$ M). In contrast to that, methyl derivative **62** was slightly less potent (β -hematin $IC_{50} = 15 \mu$ M), but a more basic core nitrogen could explain the higher NF54 activity ($IC_{50} = 0.012 \mu$ M) compared to nitrile substituted derivative **63**. The aminopiperidine **25**, which showed a high K1 cross-resistance ratio was less active in the β -hematin assay ($IC_{50} = 148 \mu$ M) relative to the frontrunner **37**, suggesting a potential mode of action in the DV. To further probe the effect of these derivatives on hemozoin formation in whole parasites, **25** was tested alongside **37** in a cell fractionation assay, which determines dose response levels of both free heme and hemozoin intracellularly. An increase in free heme with a corresponding decrease in hemozoin, correlated with parasite survival would be expected for a true hemozoin formation inhibitor. **25** showed statistically significant dose response increasing free heme and decreasing hemozoin (Figure 3), indicative of a mode of action similar to that of chloroquine. Surprisingly, no significant change in absolute free heme levels was observed with increasing concentrations of **37**. However, a decrease in hemozoin indicated that **37** could be

targeting an alternative digestive vacuole process, even though it may not be a direct hemozoin inhibitor.

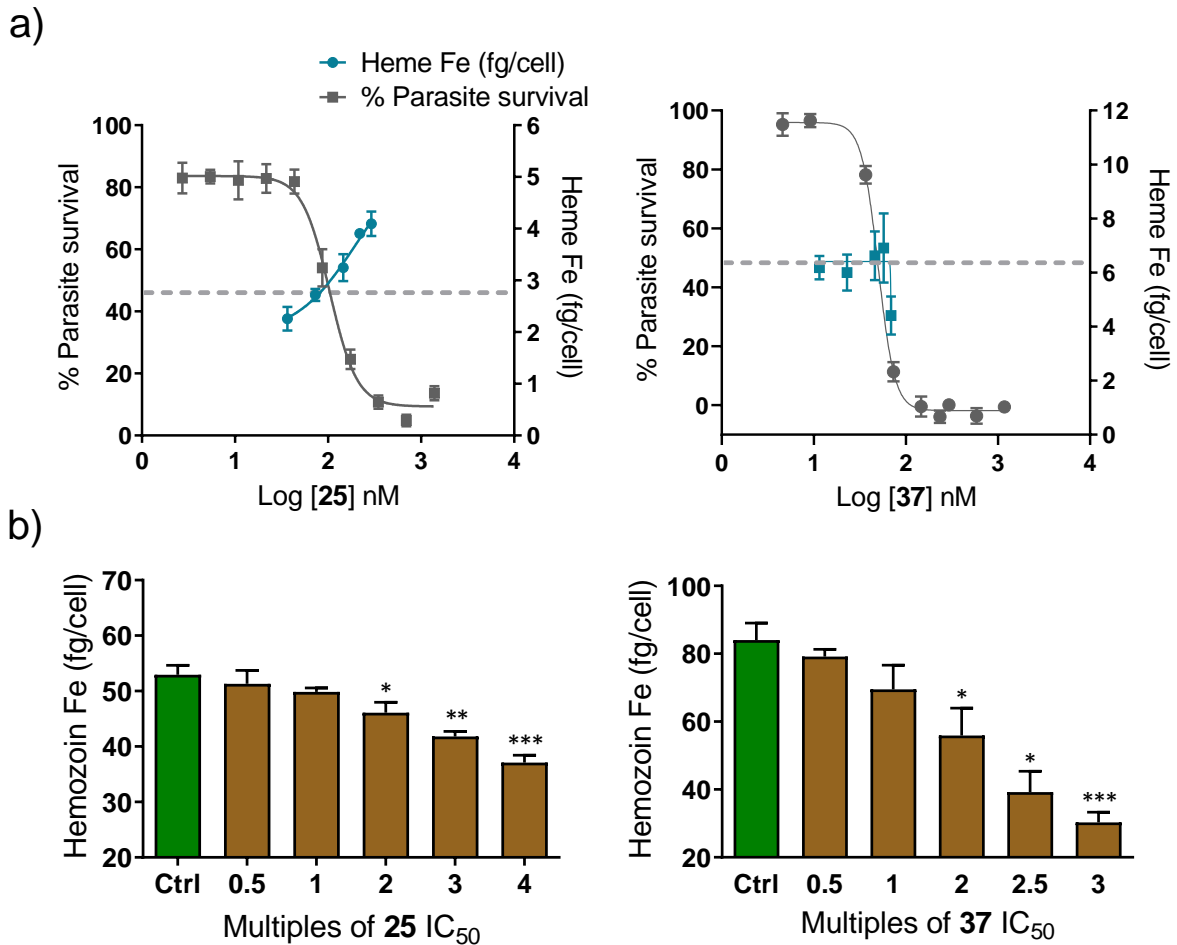


Figure 3. a) Correlation of parasite survival with intracellular free heme or b) hemozoin levels, with increasing inhibitor concentration of **25** and **37**.

***In vivo* pharmacokinetics**

Compounds that showed high NF54 activity, cytotoxicity margins and microsomal stability (Supporting Information, Table S5), were profiled for *in vivo* pharmacokinetics in mice (Table 7), to identify compounds for an *in vivo* efficacy study in a mouse model of *P. falciparum* infection (the NSG model). The selection for an *in vivo* efficacy study was made based on the best combination of having a high ratio of unbound average drug concentration to NF54 activity ($C_{av,u,24h}/NF54\ IC_{50}$) (Table 7), as well as a high cytotoxicity and hERG margin relative to NF54 activity. The $C_{av,u,24h}$ represents an approximation of the average unbound drug concentration and is determined from the unbound area under the curve (AUC_u or AUC multiplied by unbound fraction f_u) divided by the time course of the PK experiment, in this case 24 h (Supporting Information, Table S9). It provides a convenient yardstick that summarizes the aim of maximizing both drug exposure and antiplasmodium activity. Total blood clearance was low (< 30% of hepatic blood flow) to moderate for most compounds shown in Table 7, and a variable and high volume of distribution (8-96 L/kg) resulted in long plasma half-lives ranging from 6 to 26 hours. Generally, compounds showed high oral bioavailability ranging from 24% to 83%. As an exception, **19** showed low bioavailability (11%) which, despite the lowest *in vivo* intrinsic clearance of all compounds ($CL_{int} = 54\ ml/min/kg$, compare Supporting Information Table S9), limited its blood exposure. **37** showed low clearance and high oral bioavailability (83%); however, its exposure in the blood was relatively modest due to a very high volume of distribution ($V_{ss} = 37\ L/kg$). It was mainly excreted as unchanged parent in the urine and only minor metabolites were identified in mouse blood including the product of *N*-demethylation and a combination of oxidation and glucuronidation products (Supporting Information, Table S11). The *N*-demethylated metabolite **45** was equipotent against NF54 to the parent but showed 6-fold lower activity against the K1 strain. As the metabolite concentrations were minor, they were not expected to impact the activity of the

parent compound in a mouse disease model. Sustained exposure of **37** was also seen in rats with an oral bioavailability of 84% (Supporting Information, Table S8) offering confidence that PK would be similarly favorable in higher species including, most importantly, humans. It was hypothesized that renal clearance of the compound was due to a lack of reabsorption from the renal tubules since, based on pK_a predictions, it would be doubly protonated at a mouse urine pH of 6. LogD was measured to be 2.6 at pH 7.4 and is estimated to be around 0.4 at pH 6. Therefore, compounds aiming at a lower pK_a at the R¹ substituent had been synthesized but none of them showed a sufficiently good profile to be progressed into PK studies. Exemplary for the core changes with a modulated, lower core pK_a, **60** was assessed in a PK study but no improvement in clearance was observed, and, due to low activity, C_{av,u,24h}/NF54 IC₅₀ was low (0.3). While **24** was on par with **37** in terms of expected efficacy, **37** had a much superior hERG margin and was therefore assessed for *in vivo* efficacy in a NSG mouse model of *P. falciparum* infection.

Table 7. Mouse pharmacokinetic parameters calculated from non-compartmental analysis

Entry	Route	Nominal dose (mg/kg)	C _{max} (μM)	T _{max} (h)	t _{1/2} terminal (h)	mouse CL _b (mL/min/kg)	V _{ss} (L/kg)	AUC _{0-t} (min.μmol/L)	F (%)	C _{av,u,24h} /NF54 IC ₅₀
1	i.v.	2	1	-	5.9	27.3	9	215	-	
	p.o.	5	1.1	0.7	5.4	-	-	195	36	0.1
19	i.v.	2	1.7	-	8.2	11.4	4.3	406	-	
	p.o.	20	1.1	2.3	10.8	-	-	398	11	0.9
24	i.v.	2	0.3	-	25.8	19.6	20	250	-	
	p.o.	20	3.7	0.7	13.5	-	-	2074	83	4.6
32	i.v.	2	0.3	-	12.6	34.8	30	117	-	
	p.o.	20	1.5	1.5	9.8	-	-	711	61	2.5
37	i.v.	2	0.6	-	23.1	20.2	31	145	-	
	p.o.	20	1.5	1.7	32.7	-	-	1198	83	4.5
55	i.v.	2	1.6	-	12.2	9	6	473	-	
	p.o.	20	1.7	2.3	9.2	-	-	1141	24	1.5
60	i.v.	2	0.1	-	6.9	71.8	51	58	-	
	p.o.	10	0.4	3.5	4.9	-	-	214	73	0.3

i.v. intravenous; p.o. oral; CL_b blood clearance; V_{ss} volume at steady state; AUC area under the concentration-time curve from 0 h to t_{last} ; F oral bioavailability

***In vivo* efficacy studies**

37 was initially tested for efficacy in the NSG infection model via daily dosing over 4 days at 50 mg/kg three days following inoculation with *P. falciparum*. By day six post-infection, parasitemia was reduced to below the limit of detection (LOD) (Supporting Information, Scheme S1). Hence, **37** achieved an important proof-of-concept (PoC) milestone. A second study was carried out with escalating single doses of **37** at 1.5, 5, 15, 50 and 100 mg/kg (Figure 4). Parasitemia was reduced to below the LOD only at the 100 mg/kg dose, and the ED_{90} was calculated to be 62 mg/kg. The ED_{90} after a single or quadruple oral dose of chloroquine had previously been determined to ~10 mg/kg (SW personal communication) or ~5 mg/kg, respectively.²² This suggests that **37** is less potent than chloroquine. In addition, the PK analysis from the NSG infection model showed dose proportionality between 15 and 100 mg/kg and good correlation between healthy and infected mice data (Table 8). The ED_{90} dose of 62 mg/kg amounts to an approximate $AUC = 3500 \mu M \cdot min$, offering a benchmark of what would be needed to be improved with further analogue optimization work. Though **37** showed comparable activity against NF54 to compounds in clinical development including, for example, MMV390048 (NF54 $IC_{50} = 0.028 \mu M$), its exposure on PO dosing was considerably lower wherein the latter showed an $AUC = 27912 \mu M \cdot min$ on PO dosing in healthy Balb-C mice, a value over 20-fold higher.¹² Hence, less favorable PK has limited **37** from considerations for further development.

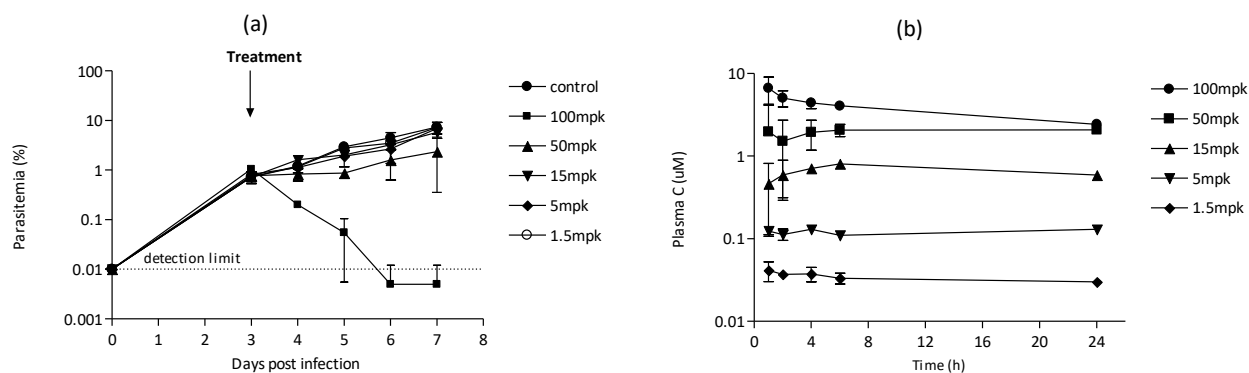


Figure 4. Results of the *in vivo* efficacy study using *P. falciparum* infected NSG mice in a single-dose regimen of **37** (a) Percent parasitemia observed after treatment (b) compound concentration in plasma over time following administration

Table 8. Pharmacokinetic data for **37** of *P. falciparum* infected NSG and healthy Balb/c mice on PO dosing

Mouse PK parameter	Dose (mg/kg)	T _{max} (h)	C _{max} (µM)	C _{max} /dose (µM.kg/mg)	AUC ₀₋₂₄ (µM·min)	AUC ₀₋₂₄ /dose (µM·min.kg/mg)
<i>P. falciparum</i> infected NSG mice	1.5	1.5	0.04	0.03*	46	31**
	5	2.5	0.13	0.03*	170	34**
	15	6.0	0.81	0.05	969	65
	50	12.5	2.84	0.06	2856	57
	100	1.0	6.68	0.07	5142	51
	4*50	4.0	2.84	0.06	3102	62
Healthy Balb/c mice	20	1.7	1.52	0.08	1198	60

Values statistically different within columns according to ANOVA (*p<0.05; **p<0.01)

Conclusion

Starting from hit compound **1**, antiplasmodium activity was improved by repositioning of the basic center using different R¹ substituents such as diazepanes and 4-aminopiperidines. However, cross-resistance against the K1 strain was observed for some compounds. During these structure activity relationship studies, tertiary amines were found to show the lowest cross-resistance ratio (NF54/K1 mostly between 1 and 4), while those of secondary and primary amines were increasingly higher (up to 16-fold). The extension of the R¹ basic center further away from the core mitigated hERG activity increasing margins from 6-fold in diazepanes to 1300-fold in **37**. Cytotoxicity could be regulated through the modulation of basicity of the R¹ substituent and the fluorine substitution pattern of the R² substituent. However, decreasing R¹ basicity was detrimental to NF54 activity thereby also compromising hERG margins. In summary, hit-to-lead progression based on structure activity relationship studies and modulation of physicochemical properties led to **37** with significantly improved *in vitro* antiplasmodium (NF54 and K1) activity, cytotoxicity SI and hERG margins (Figure 5).

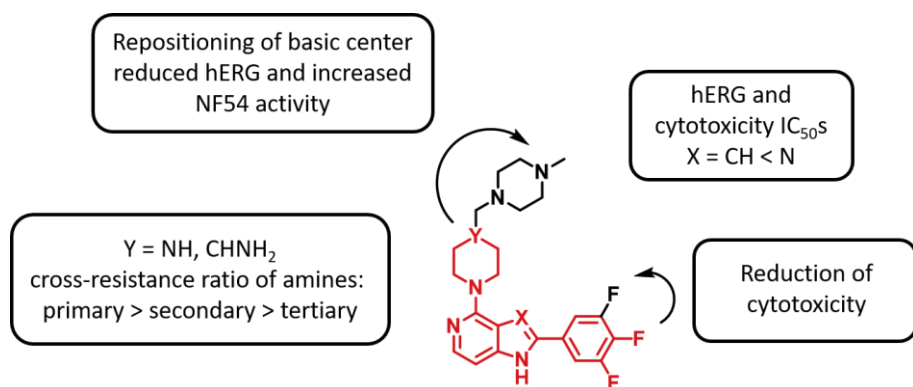


Figure 5. Summary of key SAR and SPR learnings

Compound **37** showed fast killing kinetics in the *in vitro* PRR assay. It did not show any hint of cross-resistance against panels of lab-generated resistant mutants and field isolates, which offers a clear advantage over chloroquine. With a favorable *in vitro* profile, **37** was prioritized for *in vivo* pharmacokinetic and efficacy studies, from which it demonstrated PoC in the NSG mouse model with an ED₉₀ of 62 mg/kg. Hence, **37** has considerable value as a lead antimalarial compound without issues of pre-existing resistance in the field and the potential of quick alleviation of symptomology in the clinic. Work still needs to be done to fully understand the mode of action, which would be of great value to identify an exploitable *Plasmodium* target for drug design. Initial attempts to generate drug resistant mutants using **37** were unsuccessful. These ‘irresistible’ compounds are seen as a high priority for malaria drug development since generation of resistance in the field is deemed less likely. Furthermore, improvement of PK attributes, antiplasmodium activity and/or both is still needed to deliver an optimized lead that would have a sufficiently low predicted dose in humans to warrant further development.

Experimental Section

All commercially available chemicals were purchased from either Sigma-Aldrich, Combi-Blocks, Enamine or Fluorochem. ¹H-NMR spectra were recorded on a Bruker Spectrometer at 300 MHz. ¹³C-NMR spectra were recorded either on a Bruker spectrometer at 400 MHz (¹H 400.2 MHz; ¹³C 100.6 MHz) or Bruker-600 (¹H 600.3 MHz; ¹³C 150.9 MHz). Chemical shifts (δ) are given in parts per million (ppm) referenced to the respective residual solvent peak. Coupling constants, *J*, are recorded in Hertz (Hz). Standard acronyms representing multiplicity are used as follows: br s = broad singlet, s = singlet, d = doublet, t = triplet, m = multiplet. Analytical thin-

layer chromatography (TLC) was performed on aluminum-backed silica gel 60 F254 (70–230 mesh) plates. Column chromatography was performed with Merck silica-gel 60 (70–230 mesh) using a Teledyne ISCO Combiflash Rf. Purity was determined using an Agilent LC/MS system consisting of an Agilent 1260 Infinity binary pump, Agilent 1260 Infinity diode array detector (DAD), Agilent 1290 Infinity column compartment, Agilent 1260 Infinity standard autosampler, and Agilent 6120 quadrupole (single) mass spectrometer, equipped with APCI and ESI multimode ionization source, and all compounds tested for biological activity were confirmed to have $\geq 95\%$ purity. The syntheses of building blocks and further final compounds are described in the Supporting Information.

General Procedure A for the amination

To 4-bromo-2-aryl-1*H*-imidazo[4,5-*c*]pyridine (1 eq) and the corresponding amine (2 eq) in EtOH, DIPEA (2.5 eq) was added. The mixture was stirred at 140 °C for 4.5-6 h in the microwave, cooled to 25 °C and purified by flash chromatography using a gradient of (0.5 M NH₃) MeOH in DCM to afford the desired product.

General Procedure B for the amination:

To a suspension of the 4-chloro-2-aryl-1*H*-imidazo[4,5-*c*]pyridine (1 eq) and the corresponding amine (3 eq) in minimum volume of *n*-BuOH (1.5 ml for 100 mg chloride starting material) was added DIPEA (5 eq) in a seal pressure reaction tube. The resulting reaction mixture was stirred and heated at a temperature of 140 °C. After 16 h, the mixture was cooled to 25 °C and concentrated *in vacuo*. The crude reaction mixture was purified by flash chromatography using a gradient of (0.5 M NH₃) MeOH in DCM (0-30% gradient) afforded the desired product.

2-(3,4-difluorophenyl)-4-(4-methylpiperazin-1-yl)-3H-imidazo[4,5-c]pyridine (1)

To a stirred solution of 4-bromo-2-(3,4-difluorophenyl)-1H-imidazo[4,5-c]pyridine (0.600 g, 1.93 mmol) and *N*-methyl piperazine (0.290 g, 2.90 mmol) in MeCN (10 ml) was added DIPEA (0.612 g, 4.75 mmol). The reaction mixture was irradiated at 150 °C for 3 h and the solvent evaporated under vacuum. The crude product was purified by column chromatography by using neutral alumina and 2% MeOH in DCM to yield **1**.

Yield: 0.130 g (20%). ¹H NMR (600 MHz, DMSO-*d*₆) δ 13.11 (s, 1H), 8.14 – 8.07 (m, 1H), 8.00 – 7.94 (m, 1H), 7.81 (d, *J* = 5.5 Hz, 1H), 7.63 (dt, *J* = 10.6, 8.5 Hz, 1H), 6.87 (d, *J* = 5.6 Hz, 1H), 4.11 (s, 4H), 2.46 (t, *J* = 5.0 Hz, 4H), 2.22 (s, 3H). ¹³C NMR (151 MHz, DMSO-*d*₆) δ 151.1, 150.3 (dd, *J* = 249.5, 12.4 Hz), 149.7 (dd, *J* = 246.0, 13.0 Hz), 146.0, 140.9, 140.2, 128.4, 127.3, 123.3, 118.4 (d, *J* = 17.7 Hz), 115.2 (d, *J* = 18.8 Hz), 98.4, 54.8, 45.9, 45.7. LC/MS (ESI⁺): found *m/z* = 330.2 [M+H]⁺ (calc. for C₁₇H₁₇F₂N₅ *m/z* = 330.2 [M+H]⁺).

4-(2-(3,4-difluorophenyl)-1H-imidazo[4,5-c]pyridin-4-yl)piperazin-2-one (3)

General procedure B. Yield: 50%. ¹H NMR (300 MHz, DMSO-*d*₆) δ 13.26 (s, 1H), 8.14 (ddd, *J* = 11.8, 7.8, 2.2 Hz, 1H), 7.98 (s, 1H), 7.86 (d, *J* = 5.6 Hz, 1H), 7.74 – 7.57 (m, 1H), 6.95 (d, *J* = 5.7 Hz, 1H), 4.59 (s, 2H), 4.39 (t, *J* = 5.5 Hz, 2H), 3.36 (m, 4H). LC/MS (ESI⁺): found *m/z* = 330.1 (M+H)⁺ (calc. for C₁₆H₁₃F₂N₅O *m/z* = 330.1 [M+H]⁺).

4-(2-(3,4-difluorophenyl)-1H-imidazo[4,5-c]pyridin-4-yl)morpholine (4)

General procedure A using MeCN as solvent. Yield: 22%. ¹H NMR (400 MHz, DMSO-*d*₆): δ 13.19 (s, 1H), 8.13 (t, *J* = 7.60 Hz, 1H), 7.97 (s, 1H), 7.84 (d, *J* = 5.20 Hz, 1H), 7.65 (q, *J* = 8.40

Hz, 1H), 6.93 (d, $J = 5.60$ Hz, 1H), 4.09 (t, $J = 4.40$ Hz, 4H), 3.77 (t, $J = 4.40$ Hz, 4H). LC/MS (APCI⁺): found m/z 317.0 (M+H)⁺ (calc. for C₁₆H₁₄F₂N₄O $m/z = 317.1$ [M+H]⁺).

2-(3,4-difluorophenyl)-4-(piperazin-1-yl)-1H-imidazo[4,5-c]pyridine (6)

Step 1: General procedure A. *tert*-butyl 4-(2-(3,4-difluorophenyl)-1*H*-imidazo[4,5-*c*]pyridin-4-yl)piperazine-1-carbamate. Yield: 41%. LC/MS (ESI⁺): found $m/z = 416.2$ (M+H)⁺ (calc. for C₂₁H₂₃F₂N₅O₂ $m/z = 416.2$ [M+H]⁺).

Step 2: To a suspension of *tert*-butyl 4-(2-(3,4-difluorophenyl)-1*H*-imidazo[4,5-*c*]pyridin-4-yl)piperazine-1-carbamate (58 mg, 0.140 mmol) in DCM (1 ml) was added TFA (0.1 ml) at 25 °C. After 3 h, the product was precipitated with Et₂O and desalted using an SCX-2 column.

Yield: 96%. ¹H NMR (300 MHz, DMSO-*d*₆) δ 8.10 (ddd, $J = 11.8, 7.8, 2.2$ Hz, 1H), 7.97 (m, 1H), 7.81 (d, $J = 5.5$ Hz, 1H), 7.62 (dt, $J = 10.6, 8.5$ Hz, 1H), 6.86 (d, $J = 5.6$ Hz, 1H), 4.07 – 3.98 (m, 4H), 2.94 – 2.78 (m, 4H). LC/MS (ESI⁺): found $m/z = 316.1$ (M+H)⁺ (calc. for C₁₆H₁₅F₂N₅ $m/z = 316.1$ [M+H]⁺).

*2-(3,4-difluorophenyl)-4-(hexahydropyrrolo[1,2-*a*]pyrazin-2(1*H*)-yl)-1H-imidazo[4,5-*c*]pyridine (7)*

General procedure A. Yield: 27%. ¹H NMR (300 MHz, DMSO-*d*₆) δ 8.11 (ddd, $J = 11.8, 7.7, 2.1$ Hz, 1H), 7.98 (ddd, $J = 8.8, 4.4, 1.9$ Hz, 1H), 7.82 (d, $J = 5.6$ Hz, 1H), 7.64 (dt, $J = 10.5, 8.5$ Hz, 1H), 6.87 (d, $J = 5.5$ Hz, 1H), 5.35 (d, $J = 12.4$ Hz, 2H), 3.16 – 2.99 (m, 3H), 2.73 (t, $J = 11.1$ Hz, 1H), 2.26 (s, 1H), 2.10 (d, $J = 11.6$ Hz, 2H), 1.96 – 1.79 (m, 1H), 1.79 – 1.61 (m, 2H), 1.57 – 1.33 (m, 1H). LC/MS (ESI⁺): found $m/z = 356.1$ (M+H)⁺ (calc. for C₁₉H₁₉F₂N₅ $m/z = 356.2$ [M+H]⁺).

2-(4-(2-(3,4-difluorophenyl)-1H-imidazo[4,5-c]pyridin-4-yl)piperazin-1-yl)ethan-1-ol (8)

General procedure B. Yield: 65%. ¹H NMR (300 MHz, DMSO-*d*₆) δ 8.11 (ddd, *J* = 11.8, 7.8, 2.1 Hz, 1H), 7.97 (ddt, *J* = 8.2, 3.7, 1.6 Hz, 1H), 7.82 (d, *J* = 5.6 Hz, 1H), 7.63 (dt, *J* = 10.5, 8.5 Hz, 1H), 6.88 (d, *J* = 5.6 Hz, 1H), 4.46 (s, 1H), 4.12 (t, *J* = 4.7 Hz, 4H), 3.57 (t, *J* = 6.2 Hz, 2H), 2.60 (t, *J* = 4.9 Hz, 4H), 2.53 – 2.41 (m, 3H). LC/MS (ESI⁺): found *m/z* = 360.1 [M+H]⁺ (calc. for C₁₈H₁₉F₂N₅O *m/z* = 360.2 [M+H]⁺).

2-(3,4-difluorophenyl)-4-(4-(2,2,2-trifluoroethyl)piperazin-1-yl)-1H-imidazo[4,5-c]pyridine (9)

General procedure A. Yield: 20%. ¹H NMR (300 MHz, DMSO-*d*₆) δ 8.13 (ddd, *J* = 11.7, 7.8, 2.2 Hz, 1H), 7.98 (ddt, *J* = 10.5, 3.9, 1.6 Hz, 1H), 7.82 (d, *J* = 5.7 Hz, 1H), 7.64 (dt, *J* = 10.6, 8.5 Hz, 1H), 6.92 (d, *J* = 5.7 Hz, 1H), 4.15 (t, *J* = 4.8 Hz, 4H), 3.24 (q, *J* = 10.2 Hz, 2H), 2.79 (t, *J* = 4.9 Hz, 4H). LC/MS (ESI⁺): found *m/z* = 398.1 (M+H)⁺ (calc. for C₁₈H₁₆F₅N₅ *m/z* = 398.1 [M+H]⁺).

2-(3,4-difluorophenyl)-4-(4-phenylpiperazin-1-yl)-1H-imidazo[4,5-c]pyridine (10)

General procedure A. Yield: 15%. ¹H NMR (300 MHz, DMSO-*d*₆) δ 8.13 (ddd, *J* = 11.8, 7.8, 2.2 Hz, 1H), 8.05 – 7.93 (m, 1H), 7.85 (d, *J* = 5.6 Hz, 1H), 7.64 (dt, *J* = 10.6, 8.5 Hz, 1H), 7.30 – 7.17 (m, 2H), 7.01 (d, *J* = 8.1 Hz, 2H), 6.91 (d, *J* = 5.6 Hz, 1H), 6.79 (t, *J* = 7.2 Hz, 1H), 4.27 (t, *J* = 4.9 Hz, 4H), 4.02 (s, 2H), 3.28 (2H, covered by water peak). LC/MS (ESI⁺): found *m/z* = 392.1 (M+H)⁺ (calc. for C₂₂H₁₉F₂N₅ *m/z* = 392.2 [M+H]⁺).

2-(3,4-difluorophenyl)-4-((3S,5R)-3,5-dimethylpiperazin-1-yl)-1H-imidazo[4,5-c]pyridine (11)

General procedure A. Yield: 47%. ¹H NMR (300 MHz, Methanol-*d*₄) δ 7.99 (ddd, *J* = 11.6, 7.6, 2.2 Hz, 1H), 7.91 (ddt, *J* = 8.0, 3.8, 1.7 Hz, 1H), 7.80 (d, *J* = 5.8 Hz, 1H), 7.44 (dt, *J* = 10.3, 8.4 Hz, 1H), 6.92 (d, *J* = 5.8 Hz, 1H), 5.19 – 5.05 (m, 2H), 3.03 (dtd, *J* = 12.8, 6.4, 2.8 Hz, 2H), 2.65 (dd, *J* = 12.9, 10.7 Hz, 2H), 1.22 (s, 3H), 1.20 (s, 3H). LC/MS (ESI⁺): found *m/z* = 344.2 [M+H]⁺ (calc. for C₁₈H₁₉F₂N₅ *m/z* = 344.2 [M+H]⁺).

2-(3,4-difluorophenyl)-4-((3S,5R)-3,4,5-trimethylpiperazin-1-yl)-1H-imidazo[4,5-c]pyridine (**12**)

General procedure B. Yield: 66%. ¹H NMR (300 MHz, DMSO-*d*₆) δ 13.41 (s, 1H), 8.29 – 8.13 (m, 1H), 8.02 (s, 1H), 7.89 (d, *J* = 5.6 Hz, 1H), 7.66 (dt, *J* = 10.5, 8.5 Hz, 1H), 7.01 (d, *J* = 5.6 Hz, 1H), 5.42 (d, *J* = 13.4 Hz, 2H), 3.68 – 3.55 (m, 1H), 3.40 (m, 4H) 3.17 – 3.05 (m, 1H), 2.82 (s, 3H), 1.43 (6, 5H). LC/MS (ESI⁺): found *m/z* = 358.2 [M+H]⁺ (calc. for C₁₉H₂₁F₂N₅ *m/z* = 358.2 [M+H]⁺).

4-(1,4-diazepan-1-yl)-2-(3,4-difluorophenyl)-1H-imidazo[4,5-c]pyridine (**13**)

General procedure B using Boc-diazepane. Thermal *in situ* Boc deprotection. Yield: 18%. ¹H NMR (300 MHz, DMSO-*d*₆) δ 8.14 (ddd, *J* = 11.8, 7.8, 2.1 Hz, 1H), 8.03 – 7.93 (m, 1H), 7.83 (d, *J* = 5.6 Hz, 1H), 7.66 (dt, *J* = 10.6, 8.5 Hz, 1H), 6.87 (d, *J* = 5.6 Hz, 1H), 4.37 (t, *J* = 5.1 Hz, 2H), 4.24 (t, *J* = 6.1 Hz, 2H), 3.41 (t, *J* = 5.3 Hz, 2H), 3.22 – 3.16 (m, 2H), 2.18 – 2.07 (m, 2H). **Note:** The NH proton could not be seen clearly due to water in the DMSO-*d*₆. LC/MS (ESI⁺): found *m/z* = 330.1 [M+H]⁺ (calc. for C₁₇H₁₇F₂N₅ *m/z* = 330.2 [M+H]⁺).

2-(3,4-difluorophenyl)-4-(4-methyl-1,4-diazepan-1-yl)-1H-imidazo[4,5-c]pyridine (**14**)

General procedure B. Yield: 75%. ¹H NMR (300 MHz, DMSO-*d*₆) δ 13.03 (s, 1H), 8.09 (ddd, *J* = 11.8, 7.8, 2.1 Hz, 1H), 7.95 (ddd, *J* = 8.2, 4.2, 2.0 Hz, 1H), 7.78 (d, *J* = 5.6 Hz, 1H), 7.63 (dt, *J* = 10.6, 8.5 Hz, 1H), 6.76 (d, *J* = 5.6 Hz, 1H), 4.27 (t, *J* = 4.9 Hz, 2H), 4.13 (t, *J* = 6.4 Hz, 2H), 2.78 (t, *J* = 4.8 Hz, 2H), 2.55 (d, *J* = 6.9 Hz, 2H), 2.31 (s, 3H), 2.05 – 1.95 (m, 2H). LC/MS (ESI⁺): found *m/z* = 344.1 [M+H]⁺ (calc. for C₁₈H₁₉F₂N₅ *m/z* = 344.2 [M+H]⁺).

4-(4-(cyclopropylmethyl)-1,4-diazepan-1-yl)-2-(3,4-difluorophenyl)-1H-imidazo[4,5-c]pyridine
(15)

General procedure B. Yield: 31%. ¹H NMR (300 MHz, Methanol-*d*₄) δ 8.02 (ddd, *J* = 11.5, 7.6, 2.1 Hz, 1H), 7.98 – 7.86 (m, 1H), 7.81 (d, *J* = 5.8 Hz, 1H), 7.44 (dt, *J* = 10.3, 8.4 Hz, 1H), 6.91 (d, *J* = 5.8 Hz, 1H), 4.60 – 4.41 (m, 2H), 4.22 (t, *J* = 6.3 Hz, 2H), 3.67 – 3.51 (m, 2H), 2.96 (d, *J* = 7.0 Hz, 2H), 2.48 – 2.27 (m, 2H), 1.30 (s, 1H), 1.19 – 0.84 (m, 2H), 0.82 – 0.63 (m, 2H), 0.47 – 0.30 (m, 2H). LC/MS (ESI⁺): found *m/z* = 384.2 [M+H]⁺ (calc. for C₂₁H₂₃F₂N₅ *m/z* = 384.2 [M+H]⁺).

4-(2-(3,4-difluorophenyl)-1H-imidazo[4,5-c]pyridin-4-yl)-1,4-diazabicyclo[3.2.2]nonane **(16)**

General procedure B. Yield: 34%. ¹H NMR (300 MHz, DMSO-*d*₆) δ 8.23 – 8.06 (m, 1H), 8.06 – 7.91 (m, 1H), 7.84 (d, *J* = 5.6 Hz, 1H), 7.65 (dd, *J* = 19.1, 8.6 Hz, 1H), 6.87 (d, *J* = 5.6 Hz, 1H), 5.63 – 5.44 (m, 1H), 4.70 – 4.57 (m, 2H), 3.46 – 3.40 (m, 5H), 3.21 – 3.15 (m, 2H), 2.34 – 2.15 (m, 2H), 2.15 – 1.94 (m, 2H). LC/MS (ESI⁺): *m/z* = 356.0 [M+H]⁺ (calc. for C₁₉H₁₉F₂N₅ *m/z* = 356.2 [M+H]⁺).

1-(2-(3,4-difluorophenyl)-1H-imidazo[4,5-c]pyridin-4-yl)piperidin-4-amine **(17)**

Step 1: General procedure B. Yield: 75%. ¹H-NMR (300 MHz, DMSO-*d*₆) δ 12.99 (s, 1H), 8.15 – 8.04 (m, 1H), 8.01 – 7.92 (m, 1H), 7.81 (d, *J* = 5.6 Hz, 1H), 7.63 (dt, *J* = 10.5, 8.5 Hz, 1H), 7.43

– 7.19 (m, 6H), 6.85 (d, $J = 5.6$ Hz, 1H), 5.17 (d, $J = 12.8$ Hz, 2H), 5.03 (s, 2H), 3.71 – 3.55 (m, 1H), 3.15 (t, $J = 11.6$ Hz, 2H), 1.86 (d, $J = 9.8$ Hz, 2H), 1.45 (dd, $J = 20.3, 11.3$ Hz, 2H). LC/MS (ESI⁺): found $m/z = 464.2$ [M+H]⁺ (calc. for C₂₅H₂₃F₂N₅O₂ $m/z = 464.2$ [M+H]⁺).

Step 2: To a suspension of benzyl (1-(2-(3,4-difluorophenyl)-1*H*-imidazo[4,5-*c*]pyridin-4-yl)piperidin-4-yl)carbamate (205 mg, 0.442 mmol) in MeOH (5 ml), 10% Pd/C (23 mg, 0.022 mmol) was added under nitrogen. Hydrogen was bubbled through the solution using a balloon with needle for 3.5 h. The reaction mixture was filtered through a pad of celite and washed with MeOH (3x 8 ml). The filtrate was purified by preparative HPLC and subsequently desalted using an SCX-2 column.

Yield: 45%. ¹H NMR (300 MHz, DMSO-*d*₆) δ 8.29 – 8.04 (m, 1H), 7.99 (br, 1H), 7.78 (d, $J = 4.4$ Hz, 1H), 7.71 – 7.48 (m, 1H), 6.84 (d, $J = 5.2$ Hz, 1H), 5.15 (d, $J = 11.7$ Hz, 2H), 3.10 (t, $J = 11.6$ Hz, 2H), 2.90 (br, 1H), 1.96 – 1.72 (m, 2H), 1.53 – 1.07 (m, 2H). LC/MS (ESI⁺): found $m/z = 330.1$ [M+H]⁺ (calc. for C₁₇H₁₇F₂N₅ $m/z = 330.2$ [M+H]⁺).

*2-(3,4-difluorophenyl)-4-(4-(4-methylpiperazin-1-yl)piperidin-1-yl)-1*H*-imidazo[4,5-*c*]pyridine (18)*

General procedure A. Yield: 32%. ¹H NMR (300 MHz, DMSO-*d*₆) δ 13.12 (s, 1H), 8.11 (ddd, $J = 11.8, 7.8, 2.2$ Hz, 1H), 7.98 (ddd, $J = 8.8, 4.3, 1.9$ Hz, 1H), 7.81 (d, $J = 5.5$ Hz, 1H), 7.64 (dt, $J = 10.6, 8.5$ Hz, 1H), 6.85 (d, $J = 5.6$ Hz, 1H), 5.32 (d, $J = 11.8$ Hz, 2H), 2.96 (t, $J = 12.3$ Hz, 2H), 2.33 (s, 4H), 2.15 (s, 3H), 1.88 (dd, $J = 12.1, 8.8$ Hz, 2H), 1.55 – 1.37 (m, 2H), 1.24 (d, $J = 7.4$ Hz, 1H). 4 protons hidden underneath the DMSO peak (by HH-COSY). LC/MS (ESI⁺): found $m/z = 413.2$ [M+H]⁺ (calc. for C₂₂H₂₆F₂N₆ $m/z = 413.2$ [M+H]⁺).

2-(3,4-difluorophenyl)-4-(4-(1-methylpiperidin-4-yl)piperazin-1-yl)-1H-imidazo[4,5-c]pyridine (19)

General procedure A. Yield: 46%. ¹H NMR (400 MHz, DMSO-*d*₆) δ 13.14 (s, 1H), 8.16 – 8.06 (m, 1H), 8.00 – 7.92 (m, 1H), 7.80 (d, *J* = 5.5 Hz, 1H), 7.64 (q, *J* = 9.0 Hz, 1H), 6.87 (d, *J* = 5.6 Hz, 1H), 4.08 (s, 4H), 2.83 (d, *J* = 11.1 Hz, 2H), 2.62 (t, *J* = 4.9 Hz, 4H), 2.17 (s, 4H), 1.99 – 1.86 (m, 2H), 1.77 (d, *J* = 12.3 Hz, 2H), 1.55 – 1.38 (m, 2H). ¹³C NMR (101 MHz, DMSO-*d*₆) δ 151.0, 150.3 (dd, *J* = 248.7, 12.1 Hz), 149.7 (dd, *J* = 246.3, 13.6 Hz), 146.0, 140.9, 140.2, 128.3, 127.4, 123.3, 118.4 (d, *J* = 17.5 Hz), 115.3 (d, *J* = 18.8 Hz), 98.4, 60.7, 54.7, 49.0, 46.2, 45.6, 27.7. LC/MS (ESI⁺): found *m/z* = 413.2 [M+H]⁺ (calc. for C₂₂H₂₆F₂N₆ *m/z* = 413.2 [M+H]⁺).

2-(3,4-difluorophenyl)-4-[4-(1-methyl-4-piperidyl)-1,4-diazepan-1-yl]-1H-imidazo[4,5-c]pyridine (20)

In a sealed tube, 4-(1,4-diazepan-1-yl)-2-(3,4-difluorophenyl)-1H-imidazo[4,5-*c*]pyridine **13** (113 mg, 0.340 mmol) and 1-methyl-4-piperidone (0.04 ml, 0.340 mmol) were dissolved in Ti(*i*OPr)₄ (0.12 ml, 0.410 mmol) and stirred at 25 °C for 1 h. Solid NaCNBH₃ (21.6 mg, 0.340 mmol) was then added to the reaction mixture and the reaction mixture stirred at 25 °C 18 h. The reaction mixture was then concentrated *in vacuo* and purified by flash column chromatography using a gradient of 5-20% (0.5 M NH₃) MeOH in DCM.

Yield: 118 mg (81%). ¹H NMR (300 MHz, Methanol-*d*₄) δ 8.01 (ddd, *J* = 11.6, 7.7, 2.1 Hz, 1H), 7.91 (ddt, *J* = 7.9, 4.0, 1.7 Hz, 1H), 7.75 (d, *J* = 5.9 Hz, 1H), 7.44 (dt, *J* = 10.3, 8.4 Hz, 1H), 6.86 (d, *J* = 5.9 Hz, 1H), 4.37 (t, *J* = 5.2 Hz, 2H), 4.24 (t, *J* = 6.2 Hz, 2H), 3.22 – 3.07 (m, 4H), 2.96 – 2.75 (m, 3H), 2.47 (s, 3H), 2.40 (d, *J* = 11.8 Hz, 2H), 2.11 (q, *J* = 6.0 Hz, 2H), 1.96 (d, *J* = 13.1

Hz, 2H), 1.84 – 1.63 (m, 2H). LC/MS (ESI⁺): found $m/z = 427.1$ [M+H]⁺ (calc. for C₂₃H₂₉F₂N₆ $m/z = 427.2$ [M+H]⁺).

4-[6,6-difluoro-4-(1-methyl-4-piperidyl)-1,4-diazepan-1-yl]-2-(3,4-difluorophenyl)-1H-imidazo[4,5-c]pyridine (21)

General procedure B (reaction mixture heated to 150 °C for 3 d). Yield 4%. ¹H NMR (300 MHz, Methanol-*d*₄) δ 7.99 (t, $J = 9.8$ Hz, 1H), 7.89 (br s, 1H), 7.79 (d, $J = 5.7$ Hz, 1H), 7.43 (q, $J = 8.8$ Hz, 1H), 6.88 (d, $J = 5.7$ Hz, 1H), 4.86 (d, $J = 2.5$ Hz, 2H), 4.28 (d, $J = 5.5$ Hz, 2H), 3.17 (t, $J = 5.5$ Hz, 2H), 3.01 (t, $J = 13.4$ Hz, 2H), 2.90 – 2.80 (m, 1H), 2.77 – 2.66 (m, 2H), 2.63 (s, 3H), 1.95 (d, $J = 13.4$ Hz, 2H), 1.82 – 1.66 (m, 2H), 1.45 – 1.32 (m, 2H). LC/MS (ESI⁺): found $m/z = 463.1$ [M+H]⁺ (calc. for C₂₃H₂₇F₄N₆ $m/z = 463.1$ [M+H]⁺).

2-(3,4-difluorophenyl)-4-(4-((4-methylpiperazin-1-yl)methyl)piperidin-1-yl)-1H-imidazo[4,5-c]pyridine (22)

General procedure A. Yield: 5%. ¹H NMR (300 MHz, Methanol-*d*₄) δ 8.01 (ddd, $J = 11.6, 7.7, 2.2$ Hz, 1H), 7.92 (ddt, $J = 8.0, 3.7, 1.8$ Hz, 1H), 7.77 (d, $J = 5.8$ Hz, 1H), 7.44 (dt, $J = 10.4, 8.4$ Hz, 1H), 6.91 (d, $J = 5.8$ Hz, 1H), 5.15 (d, $J = 13.1$ Hz, 2H), 3.10 (t, $J = 12.2$ Hz, 2H), 2.64 (s, 7H), 2.34 (s, 3H), 2.30 (d, $J = 6.5$ Hz, 2H), 2.01 – 1.83 (m, 3H), 1.46 – 1.28 (m, 3H). LC/MS (ESI⁺): found $m/z = 427.2$ [M+H]⁺ (calc. for C₂₃H₂₈F₂N₆ $m/z = 427.2$ [M+H]⁺).

(1-(2-(3,4-difluorophenyl)-1H-imidazo[4,5-c]pyridin-4-yl)piperidin-4-yl)(4-methylpiperazin-1-yl)methanone (23)

General procedure B. Yield: 12%. ^1H NMR (300 MHz, DMSO- d_6) δ 10.24 (s, 1H), 8.17 (t, $J = 9.8$ Hz, 1H), 8.00 (s, 1H), 7.73 (dd, $J = 23.6, 7.9$ Hz, 2H), 7.07 (s, 1H), 5.21 (d, $J = 13.0$ Hz, 2H), 3.75 – 3.25 (m, 8H), 3.12 (m, 2H), 2.80 (s, 3H), 2.33 (s, 3H), 1.94 – 1.58 (m, 4H). LC/MS (ESI $^+$): found $m/z = 441.2$ [M+H] $^+$ (calc. for $\text{C}_{23}\text{H}_{26}\text{F}_2\text{N}_6\text{O}$ $m/z = 441.2$ [M+H] $^+$).

4-((1-(2-(3,4-difluorophenyl)-1H-imidazo[4,5-c]pyridin-4-yl)piperidin-4-yl)methyl)morpholine
(24)

General procedure B. Yield: 46%. ^1H NMR (400 MHz, DMSO- d_6) δ 13.14 (s, 1H), 8.16 – 8.06 (m, 1H), 8.00 – 7.92 (m, 1H), 7.80 (d, $J = 5.5$ Hz, 1H), 7.64 (q, $J = 9.0$ Hz, 1H), 6.87 (d, $J = 5.6$ Hz, 1H), 4.08 (s, 4H), 2.83 (d, $J = 11.1$ Hz, 2H), 2.62 (t, $J = 4.9$ Hz, 4H), 2.17 (s, 3H), 2.17 – 2.11 (m, 1H), 1.99 – 1.86 (m, 2H), 1.77 (d, $J = 12.3$ Hz, 2H), 1.46 (qd, $J = 11.9, 11.3, 3.4$ Hz, 2H). ^{13}C NMR (151 MHz, DMSO- d_6) δ 151.2, 150.2 (dd, $J = 248.2, 12.1$ Hz), 149.7 (dd, $J = 245.6, 12.7$ Hz), 145.7, 140.9, 140.3, 128.3, 127.4, 123.2, 118.4 (d, $J = 17.7$ Hz), 115.1 (d, $J = 19.0$ Hz), 97.8, 66.2, 64.6, 53.8, 45.9, 32.9, 30.5. LC/MS (ESI $^+$): found $m/z = 414.2$ [M+H] $^+$ (calc. for $\text{C}_{22}\text{H}_{25}\text{F}_2\text{N}_5\text{O}$ $m/z = 414.4$ [M+H] $^+$).

1-(2-(3-(trifluoromethoxy)phenyl)-1H-imidazo[4,5-c]pyridin-4-yl)piperidin-4-amine **(25)**

Step 1: benzyl (1-(2-(3-(trifluoromethoxy)phenyl)-1H-imidazo[4,5-c]pyridin-4-yl)piperidin-4-yl)carbamate. General procedure A. Deviating from the routine workup, a few drops of MeCN were added to the crude reaction mixture, followed by 80 ml of H $_2$ O and a little MeOH to afford the product as a white precipitate. Yield: 78%. LC/MS (ESI $^+$): found $m/z = 512.2$ [M+H] $^+$ (calc. for $\text{C}_{26}\text{H}_{24}\text{F}_3\text{N}_5\text{O}_3$ $m/z = 512.2$ [M+H] $^+$).

Step 2: To benzyl (1-(2-(3-(trifluoromethoxy)phenyl)-1*H*-imidazo[4,5-*c*]pyridin-4-yl)piperidin-4-yl)carbamate (374 mg, 0.731 mmol) was added TFA (4.2 ml) and heated to 100 °C for 16 h. The TFA was removed *in vacuo*. The residue was sonicated with Et₂O and solvent was removed *in vacuo*. The yellow solid was dissolved in MeOH and purified by HPLC (NH₄OAc) and subsequently desalted using a SCX-2 column.

Yield: 67%. ¹H NMR (400 MHz, Methanol-*d*₄) δ 8.12 – 8.04 (m, 1H), 8.01 (dd, *J* = 2.4, 1.2 Hz, 1H), 7.77 (d, *J* = 5.8 Hz, 1H), 7.60 (t, *J* = 8.0 Hz, 1H), 7.37 (ddt, *J* = 8.2, 2.3, 1.1 Hz, 1H), 6.90 (d, *J* = 5.8 Hz, 1H), 5.21 – 5.09 (m, 2H), 3.13 (ddd, *J* = 13.3, 12.0, 2.5 Hz, 2H), 2.97 (tt, *J* = 10.9, 4.1 Hz, 1H), 2.03 – 1.93 (m, 2H), 1.61 – 1.43 (m, 2H). LC/MS (ESI⁺): found *m/z* = 378.1 [M+H]⁺ (calc. for C₁₈H₁₈F₃N₅O *m/z* = 378.2 [M+H]⁺).

N,N-dimethyl-1-(2-(3-(trifluoromethoxy)phenyl)-1*H*-imidazo[4,5-*c*]pyridin-4-yl)piperidin-4-amine (**26**)

General procedure A. Yield: 75%. ¹H NMR (300 MHz, DMSO-*d*₆) δ 13.20 (s, 1H), 8.16 (dt, *J* = 7.8, 1.2 Hz, 1H), 8.06 (s, 1H), 7.82 (d, *J* = 5.6 Hz, 1H), 7.70 (t, *J* = 8.0 Hz, 1H), 7.49 (ddt, *J* = 8.3, 2.4, 1.2 Hz, 1H), 6.88 (d, *J* = 5.6 Hz, 1H), 5.38 (d, *J* = 13.2 Hz, 2H), 3.06 – 2.91 (m, 2H), 2.74 (s, 1H), 2.39 (s, 6H), 2.00 – 1.88 (m, 2H), 1.58 – 1.40 (m, 2H). LC/MS (ESI⁺): found *m/z* = 406.2 [M+H]⁺ (calc. for C₂₀H₂₂F₃N₅O *m/z* = 406.2 [M+H]⁺).

4-(4-(4-methylpiperazin-1-yl)piperidin-1-yl)-2-(3-(trifluoromethoxy)phenyl)-1*H*-imidazo[4,5-*c*]pyridine (**27**)

General procedure A. Yield: 17%. The product was converted to the HCl salt for better handling. ¹H NMR (300 MHz, DMSO-*d*₆) δ 14.80 (s, 1H), 13.52 (s, 1H), 11.91 (s, 2H), 8.29 (dt, *J* = 7.9, 1.2

Hz, 1H), 8.20 (s, 1H), 7.79 (d, $J = 1.8$ Hz, 1H), 7.76 (s, 1H), 7.62 – 7.56 (m, 1H), 7.26 (d, $J = 6.9$ Hz, 1H), 5.47 (d, $J = 13.5$ Hz, 2H), 3.87 – 3.48 (m, 11H), 2.84 (s, 3H), 2.46 – 2.30 (m, 2H), 2.07 – 1.88 (m, 2H). LC/MS (ESI⁺): found $m/z = 461.2$ [M+H]⁺ (calc. for C₂₃H₂₇F₃N₆O $m/z = 461.2$ [M+H]⁺).

(1-(2-(3-(trifluoromethoxy)phenyl)-1H-imidazo[4,5-c]pyridin-4-yl)piperidin-4-yl)methanamine
(28)

Step 1: using *tert*-butyl (piperidin-4-ylmethyl)carbamate. General procedure A. Yield: 99%. LC/MS (ESI⁺): found $m/z = 492.2$ [M+H]⁺ (calc. for C₂₄H₂₈F₃N₅O₃ $m/z = 492.2$ [M+H]⁺).

Step 2: To a suspension of *tert*-butyl ((1-(2-(3-(trifluoromethoxy)phenyl)-1H-imidazo[4,5-c]pyridin-4-yl)piperidin-4-yl)methyl)carbamate (180 mg, 0.366 mmol) in DCM (2.2 ml) was added TFA (0.22 ml) and stirred for 2 h at 25 °C. Et₂O (30 ml) was added, the precipitate filtered off and desalted using an SCX-2 column.

Yield: 68%. ¹H NMR (300 MHz, DMSO-*d*₆) δ 8.16 (dt, $J = 8.0, 1.2$ Hz, 1H), 8.09 – 8.02 (m, 1H), 7.79 (d, $J = 5.6$ Hz, 1H), 7.69 (t, $J = 8.0$ Hz, 1H), 7.47 (ddt, $J = 8.2, 2.3, 1.1$ Hz, 1H), 6.84 (d, $J = 5.5$ Hz, 1H), 5.32 (d, $J = 13.0$ Hz, 2H), 2.96 (td, $J = 12.8, 2.5$ Hz, 2H), 2.47 (d, $J = 6.4$ Hz, 2H), 1.85 – 1.72 (m, 2H), 1.63 – 1.45 (m, 1H), 1.29 – 1.08 (m, 2H). LC/MS (ESI⁺): found $m/z = 392.2$ [M+H]⁺ (calc. for C₁₉H₂₀F₃N₅O $m/z = 392.2$ [M+H]⁺).

4-(4-((4-methylpiperazin-1-yl)methyl)piperidin-1-yl)-2-(3-(trifluoromethoxy)phenyl)-1H-imidazo[4,5-c]pyridine **(29)**

General procedure A. Yield: 8%. ¹H NMR (300 MHz, Methanol-*d*₄) δ 8.11 (d, $J = 8.5$ Hz, 1H), 8.03 (s, 1H), 7.78 (d, $J = 5.8$ Hz, 1H), 7.63 (dd, $J = 8.0$ Hz, 1H), 7.40 (d, $J = 8.2$ Hz, 1H), 6.92 (d,

$J = 5.9$ Hz, 1H), 5.17 (d, $J = 13.1$ Hz, 2H), 3.11 (t, $J = 12.4$ Hz, 2H), 2.55 (s, 7H), 2.31 (d, $J = 11.1$ Hz, 5H), 2.01 – 1.81 (m, 3H), 1.50 – 1.26 (m, 3H). LC/MS (ESI⁺) found $m/z = 475.2$ [M+H]⁺ (calc. for C₂₄H₂₉F₃N₆O $m/z = 475.5$ [M+H]⁺).

*2-(4-fluoro-3-(trifluoromethyl)phenyl)-4-(4-(4-methylpiperazin-1-yl)piperidin-1-yl)-1H-imidazo[4,5-*c*]pyridine (30)*

General procedure B. Yield: 49%. ¹H NMR (300 MHz, Methanol-*d*₄) δ 8.48 – 8.38 (m, 2H), 7.80 (d, $J = 5.8$ Hz, 1H), 7.52 (dd, $J = 10.1, 8.7$ Hz, 1H), 6.93 (d, $J = 5.8$ Hz, 1H), 5.28 (d, $J = 13.2$ Hz, 2H), 3.07 (dd, $J = 13.2, 11.2$ Hz, 2H), 2.85 – 2.65 (m, 4H), 2.65 – 2.40 (m, 5H), 2.30 (s, 3H), 2.07 (d, $J = 11.6$ Hz, 2H), 1.66 (qd, $J = 12.2, 4.0$ Hz, 2H). LC/MS (ESI⁺): found $m/z = 463.2$ [M+H]⁺ (calc. for C₂₃H₂₆F₄N₆ $m/z = 463.2$ [M+H]⁺).

*2-(4-fluoro-3-(trifluoromethyl)phenyl)-4-(4-(piperazin-1-yl)piperidin-1-yl)-1H-imidazo[4,5-*c*]pyridine dihydrochloride (31)*

Step 1: General procedure B using *tert*-butyl 4-(piperidin-4-yl)piperazine-1-carbamate. Yield: 90%. ¹H NMR (300 MHz, Methanol-*d*₄) δ 8.44 (d, $J = 5.8$ Hz, 1H), 8.43 – 8.38 (m, 1H), 7.80 (d, $J = 5.7$ Hz, 1H), 7.57 – 7.48 (m, 1H), 6.93 (d, $J = 5.8$ Hz, 1H), 5.29 (d, $J = 13.0$ Hz, 2H), 3.46 (t, $J = 5.1$ Hz, 4H), 3.14 – 3.01 (m, 2H), 2.68 – 2.57 (m, 5H), 2.04 (d, $J = 12.4$ Hz, 2H), 1.67 (qd, $J = 12.2, 4.0$ Hz, 2H), 1.48 (s, 9H). LC/MS (ESI⁺): found $m/z = 549.3$ [M+H]⁺ (calc. for C₂₇H₃₂F₄N₆O₂ $m/z = 549.3$ [M+H]⁺).

Step 2: To a solution of *tert*-butyl 4-(1-(2-(4-fluoro-3-(trifluoromethyl)phenyl)-1H-imidazo[4,5-*c*]pyridin-4-yl)piperidin-4-yl)piperazine-1-carbamate (138 mg, 0.252 mmol) in DCM (7 ml) was

added HCl in dioxane (4 M, 0.377 ml, 1.51 mmol). The mixture was stirred for 3 h at 25 °C, Et₂O (20 ml) was added and the precipitate filtered off and washed with Et₂O (x3).

Yield: 90% as 2.HCl. ¹H NMR (300 MHz, DMSO-*d*₆) δ 13.47 (s, 1H), 9.60 (s, 2H), 8.71 – 8.53 (m, 2H), 7.84 – 7.75 (m, 2H), 7.27 (d, *J* = 6.8 Hz, 1H), 5.44 (d, *J* = 13.6 Hz, 2H), 3.79 – 3.43 (m, 11H), 2.37 (d, *J* = 12.2 Hz, 2H), 2.06 – 1.87 (m, 2H). LC/MS (ESI⁺): found *m/z* = 449.2 [M+H]⁺ (calc. for C₂₂H₂₄F₄N₆ *m/z* = 449.2 [M+H]⁺).

*2-(3,5-difluorophenyl)-4-(4-(4-methylpiperazin-1-yl)piperidin-1-yl)-1H-imidazo[4,5-*c*]pyridine (32)*

General Procedure B. Yield: 46%. ¹H NMR (600 MHz, DMSO-*d*₆) δ 13.18 (s, 1H), 7.81 (d, *J* = 5.7 Hz, 1H), 7.80 – 7.77 (m, 2H), 7.38 (tt, *J* = 9.2, 2.4 Hz, 1H), 6.85 (d, *J* = 5.6 Hz, 1H), 5.32 (d, *J* = 13.0 Hz, 2H), 3.01 – 2.93 (m, 2H), 2.64 – 2.50 (m, 4H), 2.49 – 2.45 (m, 1H), 2.33 (s, 4H), 2.15 (s, 3H), 1.92 – 1.82 (m, 2H), 1.44 (qd, *J* = 12.2, 4.0 Hz, 2H). ¹³C NMR (101 MHz, DMSO-*d*₆) δ 162.7 (dd, *J* = 246.1, 13.6 Hz), 151.0, 145.5, 140.9, 140.7, 133.1, 128.2, 109.7 – 108.7 (m), 104.9 (t, *J* = 26.1 Hz), 98.0, 61.4, 55.1, 48.4, 45.6, 45.3, 28.0. LC/MS (ESI⁺): found *m/z* = 413.2 [M+H]⁺ (calc. for C₂₂H₂₆F₂N₆ *m/z* = 413.2 [M+H]⁺).

*3-(4-(4-(4-methylpiperazin-1-yl)piperidin-1-yl)-1H-imidazo[4,5-*c*]pyridin-2-yl)benzotrile (33)*

General Procedure B. Yield: 24%. ¹H NMR (300 MHz, Methanol-*d*₄) δ 8.45 (td, *J* = 1.7, 0.6 Hz, 1H), 8.40 (ddd, *J* = 7.9, 1.8, 1.2 Hz, 1H), 7.84 (dt, *J* = 7.7, 1.4 Hz, 1H), 7.81 (d, *J* = 5.8 Hz, 1H), 7.72 (td, *J* = 7.8, 0.6 Hz, 1H), 6.94 (d, *J* = 5.8 Hz, 1H), 5.31 (d, *J* = 13.2 Hz, 2H), 3.09 (td, *J* = 12.6, 1.8 Hz, 2H), 2.94 – 2.72 (m, 4H), 2.72 – 2.51 (m, 5H), 2.38 (s, 3H), 2.08 (d, *J* = 12.2 Hz,

2H), 1.68 (qd, $J = 12.3, 4.0$ Hz, 2H), 1.43 – 1.28 (m, 1H). LC/MS (ESI⁺): found $m/z = 402.2$ [M+H]⁺ (calc. for C₂₃H₂₇N₇ $m/z = 402.2$ [M+H]⁺).

4-(4-(4-methylpiperazin-1-yl)piperidin-1-yl)-2-(3-(methylsulfonyl)phenyl)-1H-imidazo[4,5-c]pyridine (34)

General Procedure B, Yield: 45%. ¹H NMR (300 MHz, Methanol-*d*₄) δ 8.69 (dt, $J = 1.9, 1.0$ Hz, 1H), 8.45 (ddd, $J = 7.9, 1.8, 1.1$ Hz, 1H), 8.07 (ddd, $J = 7.9, 1.9, 1.1$ Hz, 1H), 7.81 (t, $J = 7.7$ Hz, 2H), 7.81 (d, $J = 5.8$ Hz, 2H), 6.95 (d, $J = 5.8$ Hz, 1H), 5.31 (d, $J = 13.2$ Hz, 2H), 3.22 (s, 3H), 3.15 – 3.00 (m, 2H), 2.72 (s, 4H), 2.65 – 2.42 (m, 5H), 2.30 (s, 3H), 2.07 (d, $J = 11.3$ Hz, 2H), 1.66 (qd, $J = 12.2, 4.0$ Hz, 2H). LC/MS (ESI⁺): found $m/z = 455.2$ [M+H]⁺ (calc. for C₂₃H₃₀N₆O₂S $m/z = 455.2$ [M+H]⁺).

methyl 3-(4-(4-(4-methylpiperazin-1-yl)piperidin-1-yl)-1H-imidazo[4,5-c]pyridin-2-yl)benzoate (35)

General Procedure B. Yield: 17%. ¹H NMR (300 MHz, Methanol-*d*₄) δ 8.76 (t, $J = 1.8$ Hz, 1H), 8.36 (dt, $J = 7.8, 1.5$ Hz, 1H), 8.13 (dt, $J = 7.8, 1.4$ Hz, 1H), 7.81 (d, $J = 5.8$ Hz, 1H), 7.66 (t, $J = 7.8$ Hz, 1H), 6.94 (d, $J = 5.8$ Hz, 1H), 5.29 (d, $J = 13.2$ Hz, 2H), 3.07 (t, $J = 12.5$ Hz, 2H), 2.73 (s, 4H), 2.66 – 2.46 (m, 5H), 2.31 (s, 3H), 2.07 (d, $J = 12.4$ Hz, 2H), 1.68 (qd, $J = 12.4, 3.6$ Hz, 2H). LC/MS (ESI⁺): found $m/z = 435.2$ [M+H]⁺ (calc. for C₂₄H₃₀N₆O₂ $m/z = 435.3$ [M+H]⁺).

2-cyclopentyl-1-(4-methoxybenzyl)-4-(4-(4-methylpiperazin-1-yl)piperidin-1-yl)-1H-imidazo[4,5-c]pyridine (36)

Step 1: General Procedure B using PMB protected intermediate. Yield: 35%. LCMS (ESI⁺): found $m/z = 489.3$ [M+H]⁺ (calc. for C₂₉H₄₀N₆O $m/z = 489.3$ [M+H]⁺).

Step 2: A suspension of 2-cyclopentyl-1-(4-methoxybenzyl)-4-(4-(4-methylpiperazin-1-yl)piperidin-1-yl)-1*H*-imidazo[4,5-*c*]pyridine (50 mg, 0.102 mmol) in TFA (2.0 ml) was heated to 100 °C overnight, cooled to RT and concentrated *in vacuo*. The residue was purified by flash chromatography using a gradient of 0-20% (0.5 M NH₃) MeOH in DCM.

Yield: 77%. ¹H NMR (300 MHz, DMSO-*d*₆) δ 7.66 (d, *J* = 6.6 Hz, 1H), 7.09 (d, *J* = 6.5 Hz, 1H), 5.09 (d, *J* = 13.0 Hz, 2H), 3.31 (m, 3H), 3.01 (m, 9H), 2.75 (m, 4H), 2.22 – 1.42 (m, 12H). LC/MS (ESI⁺): found *m/z* = 368.9 [M+H]⁺ (calc. for C₂₁H₃₂N₆ *m/z* = 369.3 [M+H]⁺).

*2-(3,5-difluorophenyl)-4-(4-((4-methylpiperazin-1-yl)methyl)piperidin-1-yl)-1H-imidazo[4,5-*c*]pyridine (37)*

General procedure B. Yield: 22%. ¹H NMR (400 MHz, DMSO-*d*₆) δ 13.19 (s, 1H), 7.85 – 7.73 (m, 3H), 7.38 (t, *J* = 9.3 Hz, 1H), 6.83 (d, *J* = 5.6 Hz, 1H), 5.27 (d, *J* = 12.9 Hz, 2H), 2.96 (t, *J* = 12.5 Hz, 2H), 2.47 – 2.17 (m, 8H), 2.14 (s, 3H), 2.12 (d, *J* = 6.8 Hz, 2H), 1.79 (d, *J* = 12.3 Hz, 3H), 1.25 – 1.06 (m, 2H). ¹³C NMR (101 MHz, DMSO-*d*₆) δ 162.7 (dd, *J* = 246.0, 13.4 Hz), 151.2, 145.4, 141.0, 140.6, 133.2, 128.2, 109.9 – 108.2 (m), 104.8 (t, *J* = 26.0 Hz), 97.9, 64.2, 54.8, 53.1, 45.9, 45.8, 33.3, 30.6. LC/MS (ESI⁺): found *m/z* = 427.1 [M+H]⁺ (calc. for C₂₃H₂₈F₂N₆ *m/z* = 427.2 [M+H]⁺).

*2-(3-chloro-4-fluorophenyl)-4-(4-((4-methylpiperazin-1-yl)methyl)piperidin-1-yl)-1H-imidazo[4,5-*c*]pyridine (38)*

General Procedure B. Yield: 42%. ¹H NMR (400 MHz, Methanol-*d*₄) δ 8.20 (d, *J* = 7.0 Hz, 1H), 8.04 (d, *J* = 7.2 Hz, 1H), 7.75 (d, *J* = 5.7 Hz, 1H), 7.38 (t, *J* = 8.7 Hz, 1H), 6.89 (d, *J* = 5.8 Hz, 1H), 5.13 (d, *J* = 13.0 Hz, 2H), 3.07 (t, *J* = 12.6 Hz, 2H), 2.55 (s, 8H), 2.33 (s, 3H), 2.27 (d, *J* =

6.7 Hz, 3H), 1.91 (d, $J = 12.2$ Hz, 3H), 1.35 (q, $J = 12.7$ Hz, 2H). LC/MS (ESI⁺): found $m/z = 443.1$ [M+H]⁺ (calc. for C₂₃H₂₈ClFN₆ $m/z = 443.2$ [M+H]⁺).

2-(4-fluoro-3-(trifluoromethyl)phenyl)-4-(4-((4-methylpiperazin-1-yl)methyl)piperidin-1-yl)-1H-imidazo[4,5-c]pyridine (39)

General Procedure B. Yield: 45%. ¹H NMR (300 MHz, Methanol-*d*₄) δ 8.49 – 8.36 (m, 2H), 7.76 (d, $J = 5.9$ Hz, 1H), 7.51 (dd, $J = 10.3, 8.6$ Hz, 1H), 6.92 (d, $J = 5.9$ Hz, 1H), 5.16 (d, $J = 12.9$ Hz, 2H), 3.18 – 3.03 (m, 2H), 2.55 (s, 7H), 2.32 (s, 3H), 2.29 (d, $J = 6.5$ Hz, 2H), 1.93 (d, $J = 12.0$ Hz, 3H), 1.42 – 1.27 (m, 2H). LC/MS (ESI⁺): found $m/z = 477.0$ [M+H]⁺ (calc. for C₂₄H₂₈F₄N₆ $m/z = 477.2$ [M+H]⁺).

2-(3-fluoro-5-(trifluoromethyl)phenyl)-4-(4-((4-methylpiperazin-1-yl)methyl)piperidin-1-yl)-1H-imidazo[4,5-c]pyridine (40)

General Procedure B. Yield: 32%. ¹H NMR: (300 MHz, Methanol-*d*₄) δ 8.28 (s, 1H), 8.16 (dt, $J = 9.2, 2.0$ Hz, 1H), 7.74 – 7.64 (m, 2H), 7.21 (d, $J = 6.9$ Hz, 1H), 5.26 (d, $J = 13.7$ Hz, 2H), 3.64 – 3.47 (m, 7H), 3.28 (br s, 4H), 2.97 (s, 3H), 2.85 (d, $J = 7.1$ Hz, 2H), 2.39 – 2.22 (m, 1H), 2.15 (d, $J = 13.3$ Hz, 2H), 1.67 – 1.46 (m, 2H). LC/MS (ESI⁺): found $m/z = 477.1$ [M+H]⁺ (calc. for C₂₄H₂₈F₄N₆ $m/z = 477.2$ [M+H]⁺).

N,N-dimethyl-3-(4-(4-((4-methylpiperazin-1-yl)methyl)piperidin-1-yl)-1H-imidazo[4,5-c]pyridin-2-yl)benzamide (41)

General Procedure B. Yield: 25%. ¹H NMR (300 MHz, DMSO-*d*₆) δ 13.10 (s, 1H), 8.23 – 8.09 (m, 2H), 7.96 (s, 1H), 7.79 (d, $J = 5.5$ Hz, 1H), 7.61 (t, $J = 7.7$ Hz, 1H), 7.54 – 7.44 (m, 1H), 6.83 (d, $J = 5.6$ Hz, 1H), 5.30 (d, $J = 12.9$ Hz, 2H), 4.12 (t, $J = 12.6$ Hz, 2H), 3.64 (d, $J = 13.7$ Hz, 2H),

3.08 – 2.92 (m, 6H), 2.80 – 2.63 (m, 4H), 2.42 (s, 3H), 2.23 (m, 1H), 1.78 (m, 3H), 1.31 – 1.09 (m, 4H). LC/MS (ESI⁺): found $m/z = 462.2$ [M+H]⁺ (calc. for C₂₆H₃₅N₇O $m/z = 462.3$ [M+H]⁺).

2-(3-(4-(4-((4-methylpiperazin-1-yl)methyl)piperidin-1-yl)-1H-imidazo[4,5-c]pyridin-2-yl)phenoxy)ethan-1-amine (42)

General Procedure B. Yield: 8%. ¹H NMR (300 MHz, Methanol-*d*₄) δ 7.84 – 7.75 (m, 2H), 7.66 (d, $J = 6.9$ Hz, 1H), 7.54 (t, $J = 8.0$ Hz, 1H), 7.30 – 7.15 (m, 2H), 5.27 (d, $J = 13.6$ Hz, 2H), 4.46 – 4.31 (m, 2H), 3.63 – 3.41 (m, 8H), 3.22 (s, 4H), 2.96 (s, 3H), 2.80 (d, $J = 7.0$ Hz, 2H), 2.25 (s, 0H), 2.13 (d, $J = 13.6$ Hz, 2H), 1.66 – 1.46 (m, 2H). LC/MS (ESI⁺): found $m/z = 450.2$ [M+H]⁺ (calc. for C₂₅H₃₅N₇O $m/z = 450.3$ [M+H]⁺).

3-(4-(4-((4-methylpiperazin-1-yl)methyl)piperidin-1-yl)-1H-imidazo[4,5-c]pyridin-2-yl)benzoic acid (43)

General Procedure B. Yield: 25%. ¹H NMR (300 MHz, DMSO-*d*₆) δ 8.70 (d, $J = 1.8$ Hz, 1H), 8.24 (d, $J = 7.8$ Hz, 1H), 8.00 (d, $J = 7.7$ Hz, 1H), 7.78 (d, $J = 5.5$ Hz, 1H), 7.57 (t, $J = 7.7$ Hz, 1H), 6.86 (d, $J = 5.5$ Hz, 1H), 5.30 (d, $J = 13.0$ Hz, 2H), 2.98 (t, $J = 12.2$ Hz, 5H), 2.35 (m, 6H), 2.15 (s, 3H), 1.93 (d, $J = 11.7$ Hz, 2H), 1.78 (m, 2H), 1.30 – 1.11 (m, 2H). LC/MS (ESI⁺): found $m/z = 435.1$ [M+H]⁺ (calc. for C₂₄H₃₀N₆O₂ $m/z = 435.3$ [M+H]⁺).

2-cyclopentyl-4-(4-((4-methylpiperazin-1-yl)methyl)piperidin-1-yl)-1H-imidazo[4,5-c]pyridine (44)

Step 1: General Procedure B using PMB protected intermediate. Yield: 29%. LC/MS (ESI⁺): found $m/z = 503.4$ [M+H]⁺ (calc. for C₃₀H₄₂N₆O $m/z = 503.4$ [M+H]⁺).

Step 2: A suspension of 2-cyclopentyl-1-(4-methoxybenzyl)-4-(4-((4-methylpiperazin-1-yl)methyl)piperidin-1-yl)-1*H*-imidazo[4,5-*c*]pyridine (43 mg, 0.086 mmol) in TFA (2.0 ml) was heated at 100 °C overnight, cooled to 25 °C and concentrated *in vacuo*. The residue was purified by flash chromatography using a gradient of 0-25% (0.5 M NH₃) MeOH in DCM.

Yield: 89%. ¹H NMR (300 MHz, DMSO-*d*₆) δ 7.65 (d, *J* = 6.7 Hz, 1H), 7.08 (d, *J* = 6.9 Hz, 1H), 5.13 – 4.97 (m, 2H), 3.32 (m, 9H), 2.99 (m, 4H), 2.77 (m, 3H), 2.28 (m, 2H), 2.20 – 2.00 (m, 2H), 1.99 – 1.65 (m, 7H), 1.27 (d, *J* = 13.3 Hz, 3H). LC/MS (ESI⁺): found *m/z* = 382.9 [M+H]⁺ (calc. for C₂₂H₃₄N₆ *m/z* = 383.3 [M+H]⁺).

2-(3,5-difluorophenyl)-4-(4-(piperazin-1-ylmethyl)piperidin-1-yl)-1H-imidazo[4,5-c]pyridine
(45)

Step 1: General procedure B using 1-benzyl-4-(piperidin-4-ylmethyl)piperazine hydrochloride. Yield: 42%. ¹H NMR (300 MHz, DMSO-*d*₆) δ 13.16 (br s, 1H), 7.88 – 7.72 (m, 3H), 7.48 – 7.15 (m, 6H), 6.84 (d, *J* = 5.7 Hz, 1H), 5.28 (d, *J* = 12.7 Hz, 2H), 3.57 – 3.42 (m, 3H), 2.99 (t, *J* = 12.7 Hz, 2H), 2.48 – 2.31 (m, 6H), 2.27 – 2.05 (m, 2H), 1.89 – 1.69 (m, 3H), 1.27 – 0.99 (m, 3H). LC/MS (ESI⁺): found *m/z* = 503.1 [M+H]⁺ (calc. for C₂₉H₃₃F₂N₆ *m/z* = 503.3 [M+H]⁺).

Step 2: N₂ was bubbled through MeOH (10 ml) for 20 min in a two necked flask equipped with a stirrer bar. 10% Pd/C (27.5 mg, 0.026 mmol) was then carefully introduced under an inert atmosphere. Once all the powder was safely washed into the MeOH, the N₂ was removed and 4-(4-((4-benzylpiperazin-1-yl)methyl)piperidin-1-yl)-2-(3,5-difluorophenyl)-1*H*-imidazo[4,5-*c*]pyridine (130 mg, 0.259 mmol) was added to the suspension which was then stirred under H₂ atmosphere at 25 °C for 16 h. The reaction mixture was filtered through celite and washed with MeOH. After concentration *in vacuo*, the residue was purified by flash column chromatography

with an eluent of 5-15% (0.5 M NH₃) in MeOH/DCM to yield 2-(3,5-difluorophenyl)-4-(4-(piperazin-1-ylmethyl)piperidin-1-yl)-1*H*-imidazo[4,5-*c*]pyridine as an off-white solid.

Yield: 45%. ¹H NMR (300 MHz, DMSO-*d*₆) δ 14.62 (s, 1H), 9.45 (s, 1H), 7.84 (h, *J* = 5.4 Hz, 2H), 7.74 (d, *J* = 6.9 Hz, 1H), 7.47 (td, *J* = 9.2, 4.6 Hz, 1H), 7.23 (d, *J* = 6.9 Hz, 1H), 5.25-5.3 (d, 2H), 3.62 – 3.40 (m, 9H), 3.22 – 3.11 (m, 2H), 2.39 – 2.26 (m, 1H), 2.07 (d, *J* = 13.1 Hz, 2H), 1.47 (q, *J* = 11.8, 11.2 Hz, 2H), 1.22 (s, 1H). LC/MS (ESI⁺): found *m/z* = 412.9 [M+H]⁺ (calc. for C₂₂H₂₆F₂N₆ *m/z* = 413.2 [M+H]⁺).

2-(3,5-difluorophenyl)-*N*-((1*S*,4*S*)-4-(4-methylpiperazin-1-yl)cyclohexyl)-1*H*-imidazo[4,5-*c*]pyridin-4-amine (**46**) and 2-(3,5-difluorophenyl)-*N*-((1*R*,4*R*)-4-(4-methylpiperazin-1-yl)cyclohexyl)-1*H*-imidazo[4,5-*c*]pyridin-4-amine (**47**)

To a solution of 4-(4-methylpiperazin-1-yl)cyclohexanamine (128 mg, 0.650 mmol) in *n*-BuOH (2 ml) were added 4-chloro-2-(3,5-difluorophenyl)-1*H*-imidazo[4,5-*c*]pyridine (145 mg, 0.550 mmol) and DIPEA (1.14 ml, 6.55 mmol) at 25 °C. The resulting reaction mixture was heated at 140 °C for 4 d. The reaction mixture was concentrated *in vacuo* and the residue was purified by flash chromatography eluting a gradient of (0.5 M NH₃) MeOH in DCM 5:95 to 30:70 to yield two diastereoisomers, eluting first the *cis*-product **46** and then the *trans*-product **47**.

46. Yield: 7%. ¹H NMR (300 MHz, Methanol-*d*₄) δ 7.79 – 7.59 (m, 3H), 7.12 (tdd, *J* = 1.6, 3.6, 9.1 Hz, 1H), 6.88 (d, *J* = 6.2 Hz, 1H), 4.26 (br.s, 1H), 3.59 – 3.50 (m, 1H), 3.11 – 3.05 (m, 1H), 2.83 (br.s, 2H), 2.72 (br.s, 2H), 2.70 (s, 3H), 2.43 (s, 2H), 2.08 (d, *J* = 10.6 Hz, 2H), 1.89 – 1.76 (m, 4H), 1.35 – 1.26 (m, 2H), 1.18 (t, *J* = 7.0 Hz, 1H), 0.99 – 0.83 (m, 2H). LC/MS (ESI⁺): found *m/z* = 427.1 [M+H]⁺ (calc. for C₂₃H₂₈F₂N₆ *m/z* = 427.2 [M+H]⁺).

47. Yield: 16%. ¹H NMR (300 MHz, Methanol-*d*₄) δ 7.84 – 7.59 (m, 3H), 7.14 (td, *J* = 4.5, 9.0 Hz, 1H), 6.94 (d, *J* = 6.4 Hz, 1H), 3.97 (br.s, 1H), 3.01 (br.s, 8H), 2.70 (s, 3H), 2.63 (br.s, 2H), 2.28 (d, *J* = 11.2 Hz, 2H), 2.10 (s, 2H), 1.87 (t, *J* = 11.4 Hz, 2H), 1.57 (d, *J* = 12.8 Hz, 2H), 1.04 – 0.87 (m, 1H). LC/MS (ESI⁺): found *m/z* = 427.1 [M+H]⁺ (calc. for C₂₃H₂₈F₂N₆ *m/z* = 427.2 [M+H]⁺).

1-[[[(3S)-1-[2-(3,5-difluorophenyl)-1H-imidazo[4,5-c]pyridin-4-yl]piperidin-3-yl]methyl]-4-methylpiperazine (48)

General procedure B. Yield: 32%. ¹H NMR (400 MHz, DMSO-*d*₆): δ 13.15 (s, 1H), 7.80-7.82 (m, 3H), 7.40 (t, *J* = 9.08 Hz, 1H), 6.82 (d, *J* = 5.48 Hz, 1H), 5.50 (d, *J* = 11.5 Hz, 2H), 4.99 (d, *J* = 12.6 Hz, 1H), 2.93 (t, *J* = 11.4 Hz, 1H), 2.74 (t, *J* = 10.9 Hz, 1H), 2.23-2.29 (m, 8H), 2.07-2.11 (m, 4H), 1.70-1.79 (m, 3H), 1.52-1.58 (m, 1H), 1.13-1.22 (m, 1H). LC/MS (ESI⁺): found *m/z* = 427.3 [M+H]⁺ (calc. for C₂₃H₂₈F₂N₆ *m/z* = 427.2 [M+H]⁺). Specific Rotation: [+42.20°] at 25 °C (c = 0.47% solution in CHCl₃; λ = 589 nm; d = 100 mm).

11-[[[(3R)-1-[2-(3,5-difluorophenyl)-1H-imidazo[4,5-c]pyridin-4-yl]piperidin-3-yl]methyl]-4-methylpiperazine (49)

General procedure B. Yield: 2%. ¹H NMR (400 MHz, DMSO-*d*₆): δ 13.18 (s, 1H), 7.80-7.82 (m, 3H), 7.39 (t, *J* = 9.12 Hz, 1H), 6.82 (d, *J* = 5.56 Hz, 1H), 5.43-5.47 (m, 1H), 4.99-5.02 (m, 1H), 2.95-2.97 (m, 1H), 2.77 (t, *J* = 10.3 Hz, 1H), 2.28-2.40 (m, 8H), 2.16-2.21 (m, 4H), 1.70-1.80 (m, 3H), 1.52-1.55 (m, 1H), 1.18-1.23 (m, 2H). LC/MS (ESI⁺): found *m/z* = 427.4 [M+H]⁺ (calc. for C₂₃H₂₈F₂N₆ *m/z* = 427.2 [M+H]⁺). Specific Rotation: [-29.20°] at 25 °C (c = 0.34% solution in CHCl₃; λ = 589 nm; d = 100 mm).

4-((1-(2-(3,5-difluorophenyl)-1H-imidazo[4,5-c]pyridin-4-yl)piperidin-4-yl)methyl)thiomorpholine 1,1-dioxide (50)

General procedure B. Yield: 56%. ¹H NMR (300 MHz, DMSO-*d*₆) δ 13.17 (s, 1H), 7.85 – 7.73 (m, 3H), 7.45 – 7.31 (m, 1H), 6.85 (d, *J* = 5.7 Hz, 1H), 5.29 (d, *J* = 13.0 Hz, 2H), 3.12 – 3.04 (m, 5H), 3.03 – 3.00 (m, 1H), 2.93 – 2.87 (m, 4H), 2.34 (d, *J* = 6.5 Hz, 2H), 1.83 (d, *J* = 11.6 Hz, 3H), 1.27 – 1.12 (m, 2H). LC/MS (ESI⁺): found *m/z* = 462.2 [M+H]⁺ (calc. for C₂₂H₂₅F₂N₅O₂S *m/z* = 462.2 [M+H]⁺).

2-(3,5-difluorophenyl)-4-(4-((4,4-difluoropiperidin-1-yl)methyl)piperidin-1-yl)-1H-imidazo[4,5-c]pyridine (51)

General procedure B. Yield: 8.3% ¹H NMR (300 MHz, Methanol-*d*₄) δ 7.83 – 7.61 (m, 3H), 7.07 (tt, *J* = 9.0, 2.2 Hz, 1H), 6.91 (d, *J* = 5.9 Hz, 1H), 5.17 (d, *J* = 13.6 Hz, 2H), 3.11 (t, *J* = 11.9 Hz, 2H), 2.66 – 2.52 (m, 4H), 2.33 (d, *J* = 6.6 Hz, 2H), 2.10 – 1.92 (m, 6H), 1.46 – 1.31 (m, 3H). LC/MS (ESI⁺): found *m/z* = 448.2 [M+H]⁺ (calc. for C₂₃H₂₅F₄N₅ *m/z* = 448.2 [M+H]⁺).

4-((1-(2-(3,5-difluorophenyl)-1H-imidazo[4,5-c]pyridin-4-yl)piperidin-4-yl)methyl)morpholine (52)

General procedure B. Yield: 27%. ¹H NMR (300 MHz, DMSO-*d*₆) δ 13.20 (br s, 1H), 7.88 – 7.74 (m, 3H), 7.37 (tt, *J* = 9.2, 2.4 Hz, 1H), 6.86 (d, *J* = 5.7 Hz, 1H), 5.28 (d, *J* = 13.0 Hz, 2H), 4.08 – 4.01 (m, 1H), 3.65 (t, *J* = 4.6 Hz, 4H), 3.03 (t, *J* = 12.4 Hz, 2H), 2.39 – 2.26 (m, 4H), 1.95 – 1.78 (m, 3H), 1.21 (d, *J* = 10.9 Hz, 3H). LC/MS (ESI⁺): found *m/z* = 414.2 [M+H]⁺ (calc. for C₂₂H₂₅F₂N₅O *m/z* = 414.2 [M+H]⁺).

2-(3,5-difluorophenyl)-4-(4-((4-(2,2,2-trifluoroethyl)piperazin-1-yl)methyl)piperidin-1-yl)-1H-imidazo[4,5-c]pyridine (53)

General procedure B. Yield: 33%. ¹H NMR (400 MHz, DMSO-*d*₆): δ 13.16 (s, 1H), 7.78-7.81 (m, 3H), 7.39 (t, *J* = 9.16 Hz, 1H), 6.82 (d, *J* = 5.52 Hz, 1H), 5.28 (d, *J* = 12.6 Hz, 2H), 3.15 (q, *J* = 10.2 Hz, 2H), 2.97 (t, *J* = 11.8 Hz, 2H), 2.59-2.61 (m, 4H), 2.36 (br s, 4H), 2.13 (d, *J* = 6.48 Hz, 2H), 1.79 (d, *J* = 11.2 Hz, 3H), 1.13-1.19 (m, 2H). LC/MS (ESI⁺): found *m/z* = 495.4 [M+H]⁺ (calc. for C₂₄H₂₇F₅N₆ *m/z* = 495.2 [M+H]⁺).

9-(2-(3,5-difluorophenyl)-1H-imidazo[4,5-c]pyridin-4-yl)-4-methyl-1-oxa-4,9-diazaspiro[5.5]undecane (54)

Step 1: *tert*-Butyl 1-oxa-6-azaspiro[2.5]octane-6-carboxylate (2.00 g, 9.38 mmol) was dissolved in methanamine (8.83 g, 94.0 mmol), 33% solution in EtOH. The mixture was stirred at 50°C overnight and followed by TLC. Solvent was removed under reduced pressure to yield **54** as a yellowish oil which solidified upon standing.

Yield: 1.77 g (77%). ¹H NMR (300 MHz, Chloroform-*d*) δ 3.86 (d, *J* = 13.2 Hz, 2H), 3.30 – 3.09 (m, 2H), 2.70 – 2.59 (m, 2H), 2.57 (s, 2H), 2.53 (s, 3H), 1.59 (q, *J* = 2.9 Hz, 1H), 1.47 (s, 9H), 1.26 (d, *J* = 5.3 Hz, 1H).

Step 2: General procedure B. Yield: 51%. ¹H NMR (300 MHz, DMSO-*d*₆) δ 13.27 (s, 1H), 7.86 – 7.76 (m, 3H), 7.37 (tt, *J* = 9.2, 2.4 Hz, 1H), 6.85 (d, *J* = 5.6 Hz, 1H), 4.70 (dd, *J* = 13.2, 4.4 Hz, 2H), 3.76 – 3.55 (m, 4H), 2.36 (s, 2H), 2.27 (s, 2H), 2.19 (s, 3H), 1.92 (d, *J* = 13.7 Hz, 2H), 1.61 (ddd, *J* = 14.0, 10.6, 4.0 Hz, 2H). LC/MS (ESI⁺): found *m/z* = 400.1 [M+H]⁺ (calc. for C₂₁H₂₃F₂N₅O *m/z* = 400.3 [M+H]⁺).

2-(3,5-difluorophenyl)-4-[4-[[4-(1-methylimidazol-2-yl)piperazin-1-yl]methyl]-1-piperidyl]-1H-imidazo[4,5-c]pyridine (55)

General Procedure B. Yield: 24%. ¹H NMR (600 MHz, DMSO-*d*₆) δ 13.12 (s, 1H), 7.80 – 7.72 (m, 3H), 7.34 (t, *J* = 9.2 Hz, 1H), 6.82 (d, *J* = 1.5 Hz, 1H), 6.80 (d, *J* = 5.5 Hz, 1H), 6.55 (d, *J* = 1.5 Hz, 1H), 5.26 (d, *J* = 13.0 Hz, 2H), 3.39 (s, 3H), 2.97 (t, *J* = 12.4 Hz, 2H), 2.94 – 2.89 (m, 4H), 2.52 – 2.47 (m, 4H), 2.24 – 2.15 (m, 2H), 1.88 – 1.76 (m, 3H), 1.18 – 1.11 (m, 2H). ¹³C NMR (151 MHz, DMSO-*d*₆) δ 162.8 (dd, *J* = 246.3, 13.4 Hz), 151.6, 151.3, 145.4, 140.9, 140.7, 133.1, 128.3, 124.0, 118.6, 109.2 (dd, *J* = 21.6, 5.2 Hz), 105.2 – 104.6 (m), 97.8, 64.2, 53.0, 50.4, 45.9, 33.2, 31.6, 30.6. LC/MS (ESI⁺): found *m/z* = 493.2 [M+H]⁺ (calc. for C₂₆H₃₀F₂N₈ *m/z* = 493.3 [M+H]⁺).

4-(4-((4-(tert-butyl)piperazin-1-yl)methyl)piperidin-1-yl)-2-(3,5-difluorophenyl)-1H-imidazo[4,5-c]pyridine (56)

Step 1: K₂CO₃ (350 mg, 2.53 mmol), *tert*-butyl 4-(bromomethyl)piperidine-1-carboxylate (400 mg, 1.44 mmol) and 1-(*tert*-butyl)piperazine (180 mg, 1.27 mmol) were placed in MeCN (4 ml), sealed and heated at 75 °C overnight. The contents were diluted with EtOAc (100ml) and washed with H₂O (50 ml) and NH₄Cl (50 ml), dried over anhydrous MgSO₄, filtered and concentrated *in vacuo*. The residue was purified by flash column chromatography, eluting with 0-10% MeOH/DCM.

Yield: 180 mg (42%). ¹H NMR (300 MHz, Methanol-*d*₄) δ 4.07 (d, *J* = 13.2 Hz, 2H), 3.09 – 2.91 (m, 3H), 2.77 (t, *J* = 12.9 Hz, 3H), 2.70 – 2.53 (m, 3H), 2.28 (d, *J* = 6.7 Hz, 2H), 1.77 (d, *J* = 12.1 Hz, 3H), 1.47 (s, 9H), 1.27 (s, 9H), 1.17 – 0.98 (m, 3H).

Step 2: General procedure B. Yield: 10%. ¹H NMR (300 MHz, Methanol-*d*₄) δ 7.83 – 7.64 (m, 3H), 7.06 (tt, *J* = 9.0, 2.4 Hz, 1H), 6.90 (d, *J* = 5.9 Hz, 1H), 5.18 (d, *J* = 13.2 Hz, 2H), 3.19 – 3.03

(m, 2H), 2.97 – 2.78 (m, 4H), 2.70 – 2.51 (m, 3H), 2.30 (d, $J = 6.5$ Hz, 2H), 1.93 (d, $J = 13.1$ Hz, 3H), 1.50 – 1.27 (m, 3H), 1.20 (s, 9H). LC/MS (ESI⁺): found $m/z = 469.2$ [M+H]⁺ (calc. for C₂₆H₃₄F₂N₆ $m/z = 469.3$ [M+H]⁺).

***In Vitro P. falciparum* Assay.** Compounds were screened against multidrug resistant (K1) and sensitive (NF54) strains of *P. falciparum in vitro* using the modified [³H]-hypoxanthine incorporation assay and the parasite lactate dehydrogenase assay. Both assays showed excellent alignment and are fully described in the Supporting Information providing a side-by-side comparison for a selection of compounds (Table S2).

Ethics. For the *in vivo* pharmacokinetics and efficacy studies, all animal experiments performed in the manuscript were conducted in compliance with institutional guidelines.

ASSOCIATED CONTENT

Supporting Information.

The Supporting Information is available free of charge on the ACS Publications website at DOI:

Synthetic procedures of building blocks and scaffold changes and the procedures used for the *in vitro* and *in vivo* antimalarial studies as well as PK and metabolism studies (pdf)

SMILES file with NF54, K1 and cytotoxicity IC₅₀ values (csv)

AUTHOR INFORMATION

Corresponding Author

*Phone: +27-21-6502553. Fax: +27-21-65045215. E-mail: Kelly.Chibale@uct.ac.za.

ORCID

Kelly Chibale: 0000-0002-1327-4727

Notes

The authors declare no competing financial interests.

ACKNOWLEDGMENT

We thank Medicines for Malaria Ventures (MMV), South African Technology Innovation Agency (TIA) and Strategic Health Innovation Partnerships (SHIP) unit of the South African Medical Research Council (SAMRC) for financial support of this research (Project MMV09/0002). The University of Cape Town (UCT), SAMRC, and South African Research Chairs Initiative of the Department of Science and Innovation, administered through the South African National Research Foundation, are gratefully acknowledged for support (KC and the chair initiative to LMB, UID84627). At Swiss TPH, we thank Sibylle Sax and Christian Scheurer for technical assistance with the [3H]-hypoxanthine incorporation assay and Ursula Lehmann, Sibylle Sax and Christoph Fischli with the SCID mouse model. At UCT, we thank Carmen de Kock, Virgil Verhoog, and Sumaya Salie for running the antimalarial assays, Nesia Barnes and Warren Olifant for running the ADME assays, and Trevor Finch for assistance with the animal work. We thank Stephan Meister at UCSD for the test against *Pb* liver forms and Dennis Smith for advice on pharmacokinetics. We would also like to thank Syngene and TCGLS for synthetic support. TJE and ACCdS acknowledge the National Institute of Allergy and Infectious Diseases of the National Institutes of Health under Award Number R01AI143521. The content is solely the responsibility of the authors and does not necessarily represent the official views of the National Institutes of Health.

ABBREVIATIONS

ABS: asexual blood stage; ADME: Absorption, Distribution, Metabolism, Excretion; APCI: atmospheric pressure chemical ionization; β H: β -hematin; Boc: tert-butylcarbamate; carl: cyclic amine resistance locus; Cbz: benzylcarbamate; CHO cells: Chinese hamster ovarian cells; CL: clearance; cytB: cytochrome B; DCM: dichloromethane; DHODH: dihydroorotate dehydrogenase; DIPEA: diisopropylethylamine; DMSO: dimethylsulfoxide; DV: digestive vacuole; eEF2: eukaryotic elongation factor 2; ESI: electrospray ionization; hERG: human ether-a-go-go related gene; HPLC: high pressure liquid chromatography; iv: intravenous administration; LC/MS: liquid chromatography / mass spectrometry; LOD: limit of detection; MetID: metabolite identification; MLM: mouse liver microsomes; NSG: NODscidIL2R γ null; *Pb*: *Plasmodium berghei*; PCT99.9: parasite clearance time (99.9 %); PI4K: phosphatidylinositol-4-kinase; *Pf*: *Plasmodium falciparum*; pLDH: parasite lactate dehydrogenase; po: oral administration; PoC: proof of concept; PRR: parasite reduction ratio; SAR: structure activity relationship; SFK: SoftFocus Kinase; SI: selectivity index; S_NAr: nucleophilic aromatic substitution; TFA: trifluoroacetic acid; TLC: thin layer chromatography; WHO: World Health Organization;

REFERENCES

- (1) World Health Organization. *World Malaria Report 2019*. Geneva.; 2019.
- (2) Blasco, B.; Leroy, D.; Fidock, D. A. Antimalarial Drug Resistance: Linking Plasmodium Falciparum Parasite Biology to the Clinic. *Nat. Med.* **2017**, *23*, 917–928.
- (3) Conrad, M. D.; Rosenthal, P. J. Antimalarial Drug Resistance in Africa: The Calm before the Storm? *Lancet Infect. Dis.* **2019**, *19*, e338–e351.
- (4) Goldberg, D. E.; Slater, A. F. G.; Cerami, A.; Henderson, G. B. Hemoglobin Degradation in the Malaria Parasite Plasmodium Falciparum: An Ordered Process in a Unique Organelle.

Proc. Natl. Acad. Sci. U. S. A. **1990**, *87*, 2931–2935.

- (5) Ecker, A.; Lehane, A. M.; Clain, J.; Fidock, D. A. PfCRT and Its Role in Antimalarial Drug Resistance. *Trends Parasitol.* **2012**, *28*, 504–514.
- (6) Nchinda, A. T.; Le Manach, C.; Paquet, T.; González Cabrera, D.; Wicht, K. J.; Brunshwig, C.; Njoroge, M.; Abay, E.; Taylor, D.; Lawrence, N.; Wittlin, S.; Jiménez-Díaz, M.-B.; Santos Martínez, M.; Ferrer, S.; Angulo-Barturen, I.; Lafuente-Monasterio, M. J.; Duffy, J.; Burrows, J.; Street, L. J.; Chibale, K. Identification of Fast-Acting 2,6-Disubstituted Imidazopyridines That Are Efficacious in the in Vivo Humanized Plasmodium Falciparum NODscidIL2R γ Null Mouse Model of Malaria. *J. Med. Chem.* **2018**, *61*, 4213–4227.
- (7) Le Manach, C.; Paquet, T.; Wicht, K.; Nchinda, A. T.; Brunshwig, C.; Njoroge, M.; Gibhard, L.; Taylor, D.; Lawrence, N.; Wittlin, S.; Eyermann, C. J.; Basarab, G. S.; Duffy, J.; Fish, P. V.; Street, L. J.; Chibale, K. Antimalarial Lead-Optimization Studies on a 2,6-Imidazopyridine Series within a Constrained Chemical Space to Circumvent Atypical Dose-Response Curves against Multidrug Resistant Parasite Strains. *J. Med. Chem.* **2018**, *61*, 9371–9385.
- (8) Medicines for Malaria Venture (MMV). <https://www.mmv.org/research-development/information-scientists> (accessed Sept 16, 2020).
- (9) Jamieson, C.; Moir, E. M.; Rankovic, Z.; Wishart, G. Medicinal Chemistry of HERG Optimizations: Highlights and Hang-Ups. *J. Med. Chem.* **2006**, *49*, 5029–5046.
- (10) Sanz, L. M.; Crespo, B.; De-Cózar, C.; Ding, X. C.; Llergo, J. L.; Burrows, J. N.; García-Bustos, J. F.; Gamo, F. J. P. Falciparum in Vitro Killing Rates Allow to Discriminate between Different Antimalarial Mode-of-Action. *PLoS One* **2012**, *7*. <https://doi.org/10.1371/journal.pone.0030949>.
- (11) Baragaña, B.; Hallyburton, I.; Lee, M. C. S.; Norcross, N. R.; Grimaldi, R.; Otto, T. D.; Proto, W. R.; Blagborough, A. M.; Meister, S.; Wirjanata, G.; Ruecker, A.; Upton, L. M.; Abraham, T. S.; Almeida, M. J.; Pradhan, A.; Porzelle, A.; Martínez, M. S.; Bolscher, J. M.; Woodland, A.; Norval, S.; Zuccotto, F.; Thomas, J.; Simeons, F.; Stojanovski, L.; Osuna-

- Cabello, M.; Brock, P. M.; Churcher, T. S.; Sala, K. A.; Zakutansky, S. E.; Jiménez-Díaz, M. B.; Sanz, L. M.; Riley, J.; Basak, R.; Campbell, M.; Avery, V. M.; Sauerwein, R. W.; Dechering, K. J.; Noviyanti, R.; Campo, B.; Frearson, J. A.; Angulo-Barturen, I.; Ferrer-Bazaga, S.; Gamo, F. J.; Wyatt, P. G.; Leroy, D.; Siegl, P.; Delves, M. J.; Kyle, D. E.; Wittlin, S.; Marfurt, J.; Price, R. N.; Sinden, R. E.; Winzeler, E. A.; Charman, S. A.; Bebrevska, L.; Gray, D. W.; Campbell, S.; Fairlamb, A. H.; Willis, P. A.; Rayner, J. C.; Fidock, D. A.; Read, K. D.; Gilbert, I. H. A Novel Multiple-Stage Antimalarial Agent That Inhibits Protein Synthesis. *Nature* **2015**, *522*, 315–320.
- (12) Paquet, T.; Le Manach, C.; Cabrera, D. G.; Younis, Y.; Henrich, P. P.; Abraham, T. S.; Lee, M. C. S.; Basak, R.; Ghidelli-Disse, S.; Lafuente-Monasterio, M. J.; Bantscheff, M.; Ruecker, A.; Blagborough, A. M.; Zakutansky, S. E.; Zeeman, A.-M.; White, K. L.; Shackelford, D. M.; Mannila, J.; Morizzi, J.; Scheurer, C.; Angulo-Barturen, I.; Martínez, M. S.; Ferrer, S.; Sanz, L. M.; Gamo, F. J.; Reader, J.; Botha, M.; Dechering, K. J.; Sauerwein, R. W.; Tungtaeng, A.; Vanachayangkul, P.; Lim, C. S.; Burrows, J.; Witty, M. J.; Marsh, K. C.; Bodenreider, C.; Rochford, R.; Solapure, S. M.; Jiménez-Díaz, M. B.; Wittlin, S.; Charman, S. A.; Donini, C.; Campo, B.; Birkholtz, L.-M.; Hanson, K. K.; Drewes, G.; Kocken, C. H. M.; Delves, M. J.; Leroy, D.; Fidock, D. A.; Waterson, D.; Street, L. J.; Chibale, K. Antimalarial Efficacy of MMV390048, an Inhibitor of Plasmodium Phosphatidylinositol 4-Kinase. *Sci. Transl. Med.* **2017**, *9*, eaad9735. <https://doi.org/10.1126/scitranslmed.aad9735>.
- (13) Phillips, M. A.; Lotharius, J.; Marsh, K.; White, J.; Dayan, A.; White, K. L.; Njoroge, J. W.; El Mazouni, F.; Lao, Y.; Kokkonda, S.; Tomchick, D. R.; Deng, X.; Laird, T.; Bhatia, S. N.; March, S.; Ng, C. L.; Fidock, D. A.; Wittlin, S.; Lafuente-Monasterio, M.; Benito, F. J. G.; Alonso, L. M. S.; Martinez, M. S.; Jimenez-Diaz, M. B.; Bazaga, S. F.; Angulo-Barturen, I.; Haselden, J. N.; Louttit, J.; Cui, Y.; Sridhar, A.; Zeeman, A. M.; Kocken, C.; Sauerwein, R.; Dechering, K.; Avery, V. M.; Duffy, S.; Delves, M.; Sinden, R.; Ruecker, A.; Wickham, K. S.; Rochford, R.; Gahagen, J.; Iyer, L.; Riccio, E.; Mirsalis, J.; Bathurst, I.; Rueckle, T.; Ding, X.; Campo, B.; Leroy, D.; Rogers, M. J.; Rathod, P. K.; Burrows, J. N.; Charman, S. A. A Long-Duration Dihydroorotate Dehydrogenase Inhibitor (DSM265) for Prevention and Treatment of Malaria. *Sci. Transl. Med.* **2015**, *7*, 296ra111.

<https://doi.org/10.1126/scitranslmed.aaa6645>.

- (14) Meister, S.; Plouffe, D. M.; Kuhlen, K. L.; Bonamy, G. M. C.; Wu, T.; Barnes, S. W.; Bopp, S. E.; Borboa, R.; Bright, A. T.; Che, J.; Cohen, S.; Dharia, N. V.; Gagaring, K.; Gettayacamin, M.; Gordon, P.; Groessl, T.; Kato, N.; Lee, M. C. S.; McNamara, C. W.; Fidock, D. A.; Nagle, A.; Nam, T. G.; Richmond, W.; Roland, J.; Rottmann, M.; Zhou, B.; Froissard, P.; Glynne, R. J.; Mazier, D.; Sattabongkot, J.; Schultz, P. G.; Tuntland, T.; Walker, J. R.; Zhou, Y.; Chatterjee, A.; Diagana, T. T.; Winzeler, E. A. Imaging of Plasmodium Liver Stages to Drive Next-Generation Antimalarial Drug Discovery. *Science* **2011**, *334*, 1372–1377.
- (15) Stickles, A. M.; De Almeida, M. J.; Morrisey, J. M.; Sheridan, K. A.; Forquer, I. P.; Nilsen, A.; Winter, R. W.; Burrows, J. N.; Fidock, D. A.; Vaidya, A. B.; Riscoe, M. K. Subtle Changes in Endochin-like Quinolone Structure Alter the Site of Inhibition within the Cytochrome Bc1 Complex of Plasmodium Falciparum. *Antimicrob. Agents Chemother.* **2015**, *59*, 1977–1982.
- (16) Le Manach, C.; Scheurer, C.; Sax, S.; Schleiferböck, S.; Cabrera, D.; Younis, Y.; Paquet, T.; Street, L.; Smith, P.; Ding, X. C.; Waterson, D.; Witty, M. J.; Leroy, D.; Chibale, K.; Wittlin, S. Fast in Vitro Methods to Determine the Speed of Action and the Stage-Specificity of Anti-Malarials in Plasmodium Falciparum. *Malar. J.* **2013**, *12*, 424.
- (17) Le Manach, C.; Nchinda, A. T.; Paquet, T.; González Cabrera, D.; Younis, Y.; Han, Z.; Bashyam, S.; Zabiulla, M.; Taylor, D.; Lawrence, N.; White, K. L.; Charman, S. A.; Waterson, D.; Witty, M. J.; Wittlin, S.; Botha, M. E.; Nondaba, S. H.; Reader, J.; Birkholtz, L.-M.; Jiménez-Díaz, M. B.; Martínez, M. S.; Ferrer, S.; Angulo-Barturen, I.; Meister, S.; Antonova-Koch, Y.; Winzeler, E. A.; Street, L. J.; Chibale, K. Identification of a Potential Antimalarial Drug Candidate from a Series of 2-Aminopyrazines by Optimization of Aqueous Solubility and Potency across the Parasite Life Cycle. *J. Med. Chem.* **2016**, *59*, 9890–9905.
- (18) van der Watt, M. E.; Reader, J.; Churchyard, A.; Nondaba, S. H.; Lauterbach, S. B.; Niemand, J.; Abayomi, S.; van Biljon, R. A.; Connacher, J. I.; van Wyk, R. D. J.; Manach,

- C. Le; Paquet, T.; Cabrera, D. G.; Brunshwig, C.; Theron, A.; Lozano-Arias, S.; Rodrigues, J. F. I.; Herreros, E.; Leroy, D.; Duffy, J.; Street, L. J.; Chibale, K.; Mancama, D.; Coetzer, T. L.; Birkholtz, L. M. Potent Plasmodium Falciparum Gametocytocidal Compounds Identified by Exploring the Kinase Inhibitor Chemical Space for Dual Active Antimalarials. *J. Antimicrob. Chemother.* **2018**, *73*, 1279–1290.
- (19) Murithi, J. M.; Owen, E. S.; Istvan, E. S.; Lee, M. C. S.; Otilie, S.; Chibale, K.; Goldberg, D. E.; Winzeler, E. A.; Llinás, M.; Fidock, D. A.; Vanaerschot, M. Combining Stage Specificity and Metabolomic Profiling to Advance Antimalarial Drug Discovery. *Cell Chem. Biol.* **2019**, 1–14.
- (20) Lelièvre, J.; Almela, M. J.; Lozano, S.; Miguel, C.; Franco, V.; Leroy, D.; Herreros, E. Activity of Clinically Relevant Antimalarial Drugs on Plasmodium Falciparum Mature Gametocytes in an Atp Bioluminescence “Transmission Blocking” Assay. *PLoS One* **2012**, *7*, 1–8.
- (21) Sandlin, R. D.; Carter, M. D.; Lee, P. J.; Auschwitz, J. M.; Leed, S. E.; Johnson, J. D.; Wright, D. W. Use of the NP-40 Detergent-Mediated Assay in Discovery of Inhibitors of β -Hematin Crystallization. *Antimicrob. Agents Chemother.* **2011**, *55*, 3363–3369.
- (22) Jiménez-Díaz, M. B.; Mulet, T.; Viera, S.; Gómez, V.; Garuti, H.; Ibáñez, J.; Alvarez-Doval, A.; Shultz, L. D.; Martínez, A.; Gargallo-Viola, D.; Angulo-Barturen, I. Improved Murine Model of Malaria Using Plasmodium Falciparum Competent Strains and Non-Myelodepleted NOD-Scid IL2R γ null Mice Engrafted with Human Erythrocytes. *Antimicrob. Agents Chemother.* **2009**, *53*, 4533–4536.

For Table of Contents Only

